(12)

(6)

OPERATION PLUMBBOB

Neutron Flux from Selected Nuclear Devices Project 2.3

Defense Atomic Support Agency
Sandia Base, Albuquerque, New Mexico

28 April 1960 (12) 62

(9) Final rept.

Nevada Test Site
May-October 1957.

NOTICE

This is an extract of WT-1412, Operation PLUMBBOB, Project 2.3, which remains classified SECRET/RESTRICTED DATA as of this date.

Extract version prepared for:
Director
DEFENSE NUCLEAR AGENCY
Washington, D.C. 20305

(11)
1 Oct [redacted] 79

Unclassified
SECURITY CLASSIFICATION OF THIS PAGE (When Data Entered)

REPORT DOCUMENTATION PAGE		READ INSTRUCTIONS BEFORE COMPLETING FORM
1. REPORT NUMBER WT-1412 (EX)	2. GOVT ACCESSION NO.	3. RECIPIENT'S CATALOG NUMBER
4. TITLE (and Subtitle) Operation PLUMBBOB Project 2.3-Neutron Flux from Selected Nuclear Devices		5. TYPE OF REPORT & PERIOD COVERED 6. PERFORMING ORG. REPORT NUMBER
7. AUTHOR(s) Defense Atomic Support Agency Sandia Base, Albuquerque, New Mexico		8. CONTRACT OR GRANT NUMBER(s)
9. PERFORMING ORGANIZATION NAME AND ADDRESS		10. PROGRAM ELEMENT, PROJECT, TASK AREA & WORK UNIT NUMBERS
11. CONTROLLING OFFICE NAME AND ADDRESS		12. REPORT DATE 28 April 1960 13. NUMBER OF PAGES 60
14. MONITORING AGENCY NAME & ADDRESS(if different from Controlling Office)		15. SECURITY CLASS. (of this report) Unclassified 15a. DECLASSIFICATION/DOWNGRADING SCHEDULE

16. DISTRIBUTION STATEMENT (of this Report)

Approved for public release; unlimited distribution.

17. DISTRIBUTION STATEMENT (of the abstract entered in Block 20, if different from Report)

18. SUPPLEMENTARY NOTES

This report has had the classified information removed and has been republished in unclassified form for public release. This work was performed by the General Electric Company-TEMPO under contract DNA001-79-C-0455 with the close cooperation of the Classification Management Division of the Defense Nuclear Agency.

19. KEY WORDS (Continue on reverse side if necessary and identify by block number)

Atmospheric Nuclear Tests
Nevada Test Site
Operation PLUMBBOB
Neutron Flux
Spectra
Detector elements
Foil-detector system

20. ABSTRACT (Continue on reverse side if necessary and identify by block number)

The objectives of this project were to measure the neutron flux and spectra for certain selected devices being tested during Operation Plumbbob and to provide neutron flux, spectra, and dose measurements in support of other projects. A total of approximately 1,500 neutron flux measurements were made utilizing the following detector elements: gold, plutonium, neptunium, uranium and sulfur.

Beyond 300 yards from ground zero there was no variation with increasing distance of the neutron energy spectrum above the thermal energies.

The extrapolation of the straight-line portion of the curve of neutron flux times slant distance squared versus the slant distance to close-in distances was invalid, since

DD FORM 1 JAN 73 1473 EDITION OF 1 NOV 65 IS OBSOLETE

Unclassified

experimental data from Operation Plumbbob confirmed that the relationship was nonlinear at close ranges.
The foil-detector system for measuring neutron flux gave reproducible results, further verifying its suitability for use in making measurements in nuclear weapons tests.

FOREWORD

This report has had classified material removed in order to make the information available on an unclassified, open publication basis, to any interested parties. This effort to declassify this report has been accomplished specifically to support the Department of Defense Nuclear Test Personnel Review (NTPR) Program. The objective is to facilitate studies of the low levels of radiation received by some individuals during the atmospheric nuclear test program by making as much information as possible available to all interested parties.

The material which has been deleted is all currently classified as Restricted Data or Formerly Restricted Data under the provision of the Atomic Energy Act of 1954, (as amended) or is National Security Information.

This report has been reproduced directly from available copies of the original material. The locations from which material has been deleted is generally obvious by the spacings and "holes" in the text. Thus the context of the material deleted is identified to assist the reader in the determination of whether the deleted information is germane to his study.

It is the belief of the individuals who have participated in preparing this report by deleting the classified material and of the Defense Nuclear Agency that the report accurately portrays the contents of the original and that the deleted material is of little or no significance to studies into the amounts or types of radiation received by any individuals during the atmospheric nuclear test program.

ERRATA SHEET FOR WT-1412 "POSTED"

NEUTRON FLUX FROM SELECTED NUCLEAR DEVICES
(OPERATION PLUMBBOB FINAL REPORT, PROJECT 2.3)

1. Page 36, Table 3.5, Station 9-2.3-9004.12 slant range should read 195 instead of 161.

2. Page 45, Table 3.13, Station 9-2.3-9004.12 slant range at $\bar{\rho}$ = 0.82 should read 195 instead of 161, and slant range at $\bar{\rho}$ = 1.0 should read 160 instead of 132.

3. Page 46, Figure 3.5, all points plotted at a slant range of 161 yards should be deleted and replaced by:

Detector	Slant Range yd	Flux times Slant Range Squared
Au	195	1.43×10^{19}
Pu	195	8.48×10^{19}
Np	195	3.73×10^{19}
U	195	9.66×10^{18}
S	195	3.88×10^{18}

4. Page 49, Figure 3.16, the point plotted at 161 yards slant range should be replaced with a point at 195 yards slant range with a value for flux times slant range squared of 1.50×10^{11}.

5. Page 50, Figure 3.17, the point plotted at a slant range of 161 yards on the $\bar{\rho}$ = 0.82 line should be replotted at a slant range of 195 yards. The point plotted at a slant range of 132 yards should be replotted at a slant range of 160 yards.

USAEC OFFICE OF TECHNICAL INFORMATION EXTENSION, P. O. BOX 401, OAK RIDGE, TENNESSEE

FOREWORD

This report presents the final results of one of the 46 projects comprising the military-effect program of Operation Plumbbob, which included 24 test detonations at the Nevada Test Site in 1957.

For overall Plumbbob military-effects information, the reader is referred to the "Summary Report of the Director, DOD Test Group (Programs 1–3)," ITR–1445, which includes: (1) a description of each detonation, including yield, zero-point location and environment, type of device, ambient atmospheric conditions, etc.; (2) a discussion of project results; (3) a summary of the objectives and results of each project; and (4) a listing of project reports for the military-effect program.

ABSTRACT

The objectives of this project were to measure the neutron flux and spectra for certain selected devices being tested during Operation Plumbbob and to provide neutron flux, spectra, and dose measurements in support of other projects. A total of approximately 1,500 neutron flux measurements were made utilizing the following detector elements: gold, plutonium, neptunium, uranium, sulfur and

For Shots Franklin, Wilson, Laplace, and Owens the measured dose values exceeded the predicted values obtained by use of the neutron dose curves of TM 23-200 by factors of 2.4, 2.9, 3.0, and 5.6, respectively. For Shot Priscilla, the measured dose was lower than the predicted dose by a factor of 1.2.

Beyond 300 yards from ground zero there was no variation with increasing distance of the neutron energy spectrum above the thermal energies.

The extrapolation of the straight-line portion of the curve of neutron flux times slant distance squared versus the slant distance to close-in distances was invalid, since experimental data from Operation Plumbbob confirmed that the relationship was nonlinear at close ranges.

The foil-detector system for measuring neutron flux gave reproducible results, further verifying its suitability for use in making measurements in nuclear weapons tests.

PREFACE

The authors wish to express appreciation for the efforts of all personnel who were assigned to this project. The efforts of these individuals were instrumental to the satisfactory completion of the project. Special mention is made of James L. Tarbox, who was responsible for all field work for Project 2.3 and whose efforts were invaluable to this project.

The authors wish to acknowledge Wendell Biggers, of the Los Alamos Scientific Laboratory, for counting assistance rendered at the test site, and Payne Harris and Joseph Sayeg, also of the Los Alamos Scientific Laboratory, for invaluable aid and service rendered during calibration of equipment and detectors at their laboratory.

CONTENTS

FIGURES

TABLES

Chapter 1
INTRODUCTION

1.1 OBJECTIVES

The objectives of Project 2.3 in Operation Plumbbob were to: (1) measure the neutron flux versus ground range for selected nuclear devices, and (2) provide neutron flux and dose measurements as required in support of other projects.

1.2 BACKGROUND

Only a portion of the neutrons produced during a nuclear detonation are utilized in maintaining the fission process. The remaining neutrons are either absorbed by the material of the device or pass into the surrounding medium. Physical measurements of the neutrons that pass into the surrounding medium as a function of distance from point of detonation have been made during all nuclear-weapon tests beginning with Operation Sandstone (References 1 through 12). General areas of interest for making these measurements were: (1) diagnostic measurements for the evaluation of the operation of the nuclear device under consideration, and (2) measurements for the evaluation of the effects of neutrons on material external to the device. This report is directed to the latter area of interest.

Of prime importance to the investigation of the effects of neutrons from a device is the establishment of the number and energy of the neutrons. The measurement of these parameters is called neutron-flux measurements in this report, and the prime objective of this project was to perform these measurements during Operation Plumbbob.

In general, two types of neutron flux measurements have been made during nuclear-weapon tests. The first, made in good geometry (i.e., where the neutron beam was collimated) was made during Operation Greenhouse (Reference 10) and Operation Upshot-Knothole (Reference 11). The second type of flux measurement was made in poor geometry (i.e., where the uncollimated beam was measured). This type of measurement has been made at nearly all test operations. It can also be said that neutron-flux measurements made prior to Operation Teapot consisted mainly of measurements of thermal neutrons, using gold as a detector, and fast neutrons above 3 Mev, using sulfur as a detector.

During Operation Upshot-Knothole (Shot 10), a high neutron flux was realized [redacted] thus necessitating the investigation of a neutron-produced dose, which could be a major casualty-producing effect of this type of weapon.

Investigations into the biological effects of neutrons necessitated the development of additional detectors that would be sensitive in the interesting region between thermal energy neutrons and 3-Mev neutrons. Culmination of these investigations was the development of fission-threshold detectors (Reference 13).

[redacted]

Generally, neutron flux measurements have involved the use of devices that detect the total (i.e., time integrated) neutron flux from a nuclear detonation. These detectors consist of small disks of selected materials for which there are (n, γ), (n, p), (n, 2n), or (n, fission) reactions of desired threshold energy and with high cross section for occurrence.

In the case of thermal neutrons, activation is effected by exposing to the neutron flux two gold foils: one bare, the other shielded by cadmium. The cadmium is of sufficient thickness to absorb the thermal neutrons. The difference of the resulting activation of these two foils is a measure of the neutron flux below the cadmium resonance peak. The measured flux below 0.3 ev is referred to as the thermal-neutron flux in this report. This method is known as the cadmium difference technique.

In the case of nonthermal neutrons, those neutrons having an energy greater than a particular energy E_i will cause a particular reaction in specific detectors, the total number of reactions produced being proportional to the number of neutrons.

By successive subtraction of the fluxes measured by the specific detectors, it is possible to obtain an indication of the neutron spectrum. Also, by placing groups of these detectors at various distances from ground zero, information may be gathered about the relationship between the neutron flux and spectrum versus distance from ground zero.

Table 1.1 lists the materials generally used with the type of activation and threshold energy E_i.

Previous work with these devices has indicated that, within experimental error, the following conclusions can be reached: (1) the flux from a detonation of a nuclear device

(2) with boosted and nonboosted devices,

TABLE 1.1 NEUTRON DETECTORS

Detector	Threshold Energy, E_i	Reaction
Gold	Thermal energies up to 0.3 ev	Au^{197} (n, α) Au^{198}
Pu^{239}	10 kev (w/B^{10} shield) *	Fission
Np^{237}	0.63 Mev *	Fission
U^{238}	1.5 Mev	Fission
Sulfur	3.0 Mev	S^{32} (n,p) P^{32}

* These values reflect the latest changes in the fission cross-section values for these materials and therefore are different from those presented in the ITR. Additionally, they also reflect the latest B^{10}(n, α) Li^7 cross-section values presented in Reference 6.

the shape of the neutron spectrum, excluding the thermal neutrons, does not change appreciably with distance from ground zero; (3) with certain small devices, the neutron hazard at distances close to ground zero may be greater than other detonation effects (i.e., gamma radiation, thermal, and blast effects).

From the aforementioned neutron-spectrum indications, it is possible to determine the tissue dose associated with the total measured neutron flux. In past experiments, a curve for first-collision tissue dose (Reference 13) has been used to relate the energy of the neutron to its dose contribution. Figure 1.1 is the plot of dose for 1 neutron/cm^2 as a function of energy (Reference 13). This curve is based on the assumption that all energy of the neutron is transferred in its first collision.

By applying the dose per neutron per square centimeter at the average energy between the effective thresholds of the detector system to the corresponding indicated fluxes, the following relationship was derived (Reference 13):

$$D = \left[0.029\, N_t + 1.0\, (N_{Pu} - N_{Np}) + 2.5\, (N_{Np} - N_U) + 3.2\, (N_U - N_S) + 3.9\, N_S \right] \times 10^{-9} \qquad (1.1)$$

Where D is the tissue dose in rep, N_t is the thermal flux; and N_{Pu}, N_{Np}, N_U, and N_S are the number of neutrons per square centimeter above the threshold for plutonium, neptunium, uranium, and sulfur, respectively. The coefficients used gave good agreement with results obtained using a Hurst proportional counter to measure neutron dose (Reference 14).

Another term is added in the case of a boosted device, because of the introduction of [illegible] to measure the very-high-energy neutrons.

Equation 1.1 would then be written:

$$D = \left[0.029\, N_t + 1.0\,(N_{Pu} - N_{Np}) + 2.5\,(N_{Np} - N_U) + 3.2\,(N_U - N_S) + 5.3\,(N_S - N_{Zr}) + 6.5\, N_{Zr} \right] \times 10^{-9} \quad (1.2)$$

Where the coefficient for the $(N_S - N_{Zr})$ term is determined in the aforementioned manner.

[redacted]

Preliminary results were obtained using the above system during Operation Castle (Reference 7). The complete system was used successfully during Operation Teapot by the Civil Effects Test Group Project 39.7 (Reference 9) and Naval Research Laboratory Project 2.2 (Reference 8),

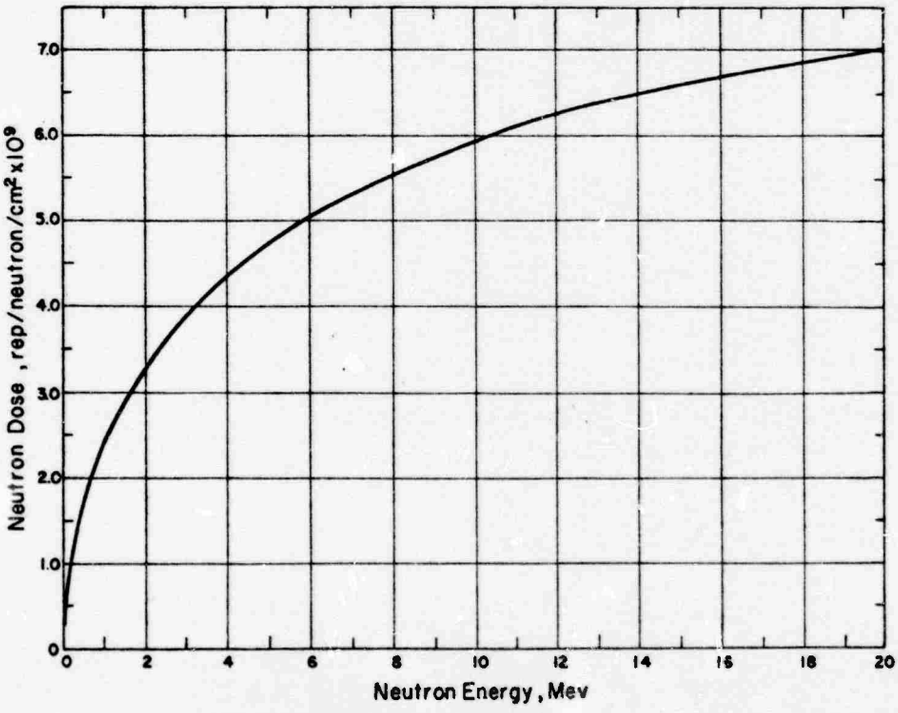

Figure 1.1 Neutron dose as a function of energy.

and during Operation Redwing by CWL Project 2.51 (Reference 1).

Chemical dosimeters have also been used to measure the neutron dose during previous operations (References 1 and 9).

1.3 THEORY

As has been discussed above, the source of the neutrons is the fission or the fusion process, depending on device design. Not all the neutrons produced are utilized in the propagation of the

reaction; hence, a certain portion of the neutrons are available to escape to the surrounding medium. In passing through the material of the device, a fraction of these neutrons are absorbed or scattered by the material. The phenomena of absorption completely remove the neutrons from the system, while that of scattering generally degrades the energy of the neutrons and changes the angular distribution. As the neutrons pass into the air, the absorption and scattering processes continue; therefore, by the time the neutrons reach any given volume in space outside the nuclear device, the number of neutrons and the energy of the individual neutrons may in no way resemble those originally produced in the nuclear reaction.

In order to theoretically explain the air scattering of neutrons emitted by the detonation of a nuclear device, diffusion or transport descriptions have been attempted which give an apparently reasonable explanation of the empirical data.

The neutron distribution is characterized by the quantity $N'(\bar{r}, \bar{\alpha}, t)$, which represents the solid angular density of neutrons at point $\bar{r}$ and flowing in the direction of unit vector $\bar{\alpha}$ about this point. The space density of neutrons at $\bar{r}$, which is $N(\bar{r}, t)$ is merely the integral of $N'(\bar{r}, \bar{\alpha} t)$ over all angles $\bar{\alpha}$.

Assuming equilibrium conditions and monoenergetic neutrons everywhere, the equation of continuity may be written:

$$\operatorname{div}\left[v\,\bar{\alpha}\,N'(\bar{r}, \bar{\alpha})\right] = \rho'(\bar{r}, \bar{\alpha}) - v\,\mu\,N'(\bar{r}, \bar{\alpha}) \tag{1.3}$$

Where: v = the magnitude of the velocity of the neutrons assumed constant

ρ' = the spatial and angular source density

μ = absorption cross section of the medium

Equation 1.3 may be solved (Reference 15) for the special case of a point isotropic source located at the origin, yielding

$$N(r) = \frac{e^{-\mu r}}{4\pi r^2 v} \tag{1.4}$$

Hence, the neutron flux, $vN(r)$, times r^2 is logarithmically linear. In previous reports on the neutron flux from nuclear detonations (References 5, 6, and 7), this special case of a point isotropic source in spherical geometry has been tacitly used as a basis of description of the flux using the nuclear device as a point source. However, it is to be noted that the above description does not include scattering in its formulation.

A characterization that is not restricted to the above assumption of constant neutron velocity may be obtained by rewriting Equation 1.3 so that N' and ρ', in addition to having a spatial and angular density, also have a lethargy density, where the lethargy, u, is defined as:

$$u = \ln\frac{E_0}{E} \tag{1.5}$$

Where: E_0 = the initial energy of the neutron

E = the energy of the neutron at the time under consideration

The domain of N', μ, and ρ' in equation 1.3 must also be expanded to include u. Furthermore, scattering may be incorporated on the right-hand side of Equation 1.3 by incorporating the term:

$$\int_0^u du \int d\bar{\alpha}'\; v\,N'(\bar{r}, \bar{\alpha}', u')\,\mu_s\,u'\;f(\bar{\alpha}' - \bar{\alpha}, u - u') \tag{1.6}$$

Where: μ_s = the scattering cross section

f = the relative probability of a neutron with lethargy u' and traveling in the direction $\bar{\alpha}'$, will, after scattering collision, travel with lethargy u and in the direction $\bar{\alpha}$.

The resulting equation obtained by the above substitutions, may be solved by expanding N′ in a series of Legendre polynomials in $\bar{\alpha}$.

Numerical results have been obtained (Reference 16), using a point isotropic source of monoenergetic neutrons, giving the contribution of a given point source at energy E_i to the total scattered flux arriving at a detector having a threshold response at energy E_t. These results were weighted with a normalized fission curve, giving the neutron flux from a fission source as a function of distance and threshold energy E_t. This was added to the contribution of neutrons coming directly from the device, (i.e., nonscattered neutrons) giving the total flux above energy E_t arriving at a detector (Reference 17).

From an examination of the functions used in the calculations, it is apparent that a definite peak in the quantity vNr^2 occurs at an ≤ 300 yards for detectors of all thresholds. Beyond r = 1,000 yards, the results show that vNr^2 becomes approximately proportional to $e^{-\mu r}$, i.e., logarithmically linear, remindful of Equation 1.4. It is pointed out that due to the peak and resulting curvature of vNr^2 at around 300 yards, logarithmically linear extrapolation back to r = 0 yards is hazardous.

In a method similar to that outlined above, the neutron spectrum from a fission source was calculated as two values of r (Reference 17). Results indicated (1) from epithermal to 0.1 Mev, the spectrum varies as E^{-1}, and (2) for larger energies, the usual fission spectrum predominates.

Neglected in the formulation are perturbations due to (1) the effect of the terrain over which the detectors were placed, (2) the components of the device surrounding the fissionable material, and (3) in the detectors, the finite domain of the step function of the threshold response.

Chapter 2
PROCEDURE

2.1 SHOT PARTICIPATION; STATION DESIGN AND LOCATION

Project 2.3 participated in a total of nine shots during Operation Plumbbob (Table 2.1).

Five of the shots in which Project 2.3 participated were selected to fulfill the requirements of the primary objective of this project, namely, to measure the neutron flux versus ground range of selected nuclear devices. These devices were those used for Shots Franklin, Lassen, Priscilla, Owens, and Laplace.

Participation in all other shots except Shot Smoky were support efforts for other projects. Because of the unique conditions under which Shot Smoky was detonated, it was possible to determine, at least generally, the effect of terrain on neutron flux versus range; therefore, Project 2.3 participation was warranted. Inherent in Shots Wilson and Smoky were measurements which were applicable to flux versus slant range experiments, and the data were handled accordingly.

In general, wherever the measurements included flux versus distance, a $^3/_4$-inch wire cable was laid along the axis at which the highest neutron flux was anticipated. Using wire rope clamps, the detectors were attached to this cable at varying distances from ground zero. Each station consisted of a gold detector, a composite fission detector, and a sulfur detector.

As is shown in Figure 2.1, each station was elevated slightly, giving each detector a clear line of sight to the point of detonation. Recovery of the detectors was effected by using a tractor or truck to pull the cable out of the surrounding high radiation field. The detector holders were then detached from the cable and returned to the laboratory trailer, located near the control point, where the samples were removed from the holders and counted.

The station locations and the projects supported are presented in subsequent sections.

2.1.1 Shot Franklin. A cable line was installed which extended due east of ground zero, a position that was clear of all shielding around the device. All data pertinent to these stations are included in Table 2.2.

In addition, 17 complete sets of detectors were required by Project 2.4 for use in neutron-shielding studies. These detectors were emplaced in M-48 tanks, Ontos vehicles, and steel armor hemispheres. Installation and recovery were effected by Project 2.4 personnel.

2.1.2 Shot Lassen. Project 2.3 participation in Shot Lassen consisted of a line of stations at 100-yard intervals from 100 to 1,000 yards running at an azimuth of 168 degrees. Table 2.3 contains all station information.

In addition, detectors were supplied to Project 2.4 for neutron-shielding studies. Support was identical to that given during Shot Franklin.

Further support was provided to Project 2.10 in their investigation of the difference in the results of neutron measurements taken at various heights above the ground. To obtain these measurements, detectors were attached to cables supported by balloons.

2.1.3 Shot Wilson. Again, Project 2.4 requested support for their neutron-shielding studies. This support was identical to that given for Shot Franklin.

Detectors were also supplied to Sandia Corporation's Project 41.3 for the measurement of neutron flux at various heights above the ground. Table 2.4 shows the location of these stations.

Project 2.10 was supplied with seventeen sulfur samples for the studies of neutron flux versus height above ground.

TABLE 2.1 PROJECT 2.3 PARTICIPATION DURING OPERATION PLUMBBOB

Shot	Date	Device	Yield	Height of Burst	Support	Area	Sponsor
			kt	ft			
Franklin	2 June		0.138	300	Tower	3	LASL
Lassen	5 June		0.47×10^{-3}	500	Balloon	9	UCRL
Wilson	18 June		10.3	500	Balloon	9	UCRL
Priscilla	24 June		36.6	700	Balloon	FF	DOD
Hood	5 July		74.3	1,500	Balloon	9	UCRL
Owens	25 July		9.6	500	Balloon	9	UCRL
John	19 July		1.73	14,850	Rocket	YUCCA	DOD
Smoky	31 Aug		43.71	700	Tower	2C	UCRL
Laplace	8 Sept		1.22	750	Balloon	7	LASL

TABLE 2.2 PROJECT 2.3 STATIONS, SHOT FRANKLIN

Station Number	Radial Distance from Ground Zero	Slant Range	Description
	yd	yd	
3-2.3-9001.01	123	158	Au, Pu, Np, U, S
3-2.3-9001.02	194	218	Au, Pu, Np, U, S
3-2.3-9001.03	312	327	Au, Pu, Np, U, S
3-2.3-9001.04	426	437	Au, Pu, Np, U, S
3-2.3-9001.05	538	547	Au, Pu, Np, U, S
3-2.3-9001.06	649	656	Au, Pu, Np, U, S
3-2.3-9001.07	759	766	Au, Pu, Np, U, S
3-2.3-9001.08	870	876	Au, Pu, Np, U, S
3-2.3-9001.09	980	985	Au, Pu, Np, U, S
3-2.3-9001.10	1,090	1,094	Au, Pu, Np, U, S

TABLE 2.3 PROJECT 2.3 STATIONS, SHOT LASSEN

Station Number	Radial Distance from Ground Zero	Slant Range	Description
	yd	yd	
9-2.3-9004.01	100	195	Au, Pu, Np, U, S
9-2.3-9004.02	200	260	Au, Pu, Np, U, S
9-2.3-9004.03	300	343	Au, Pu, Np, U, S
9-2.3-9004.04	400	433	Au, Pu, Np, U, S
9-2.3-9004.05	500	527	Au, Pu, Np, U, S
9-2.3-9004.06	600	623	Au, Pu, Np, U, S
9-2.3-9004.07	700	720	Au, Pu, Np, U, S
9-2.3-9004.08	800	817	Au, Pu, Np, U, S
9-2.3-9004.09	900	915	Au, Pu, Np, U, S
9-2.3-9004.10	1,000	1,014	Au, Pu, Np, U, S

Figure 2.1 Typical neutron-detector installation.

TABLE 2.4 PROJECT 41.3 STATIONS, SHOT WILSON

Station Number	Radial Distance from Ground Zero	Height above Ground	Slant Range	Description
	yd	yd	yd	
9-41-7001.01	0	0	167	Au, S
9-41-7001.01F	200	0	260	Pu, Np, U
9-41-7001.02	100	17	211	Au, S
9-41-7001.03	317	0	358	Au, Pu, U, S
9-41-7001.04	300	78	313	Au, S
9-41-7001.05	300	156	300	Au, S
9-41-7001.06	300	233	312	Au, S
9-41-7001.07	577	0	601	Au, Pu, U, Np, S
9-41-7001.08	600	100	604	Au, Pu, U, S
9-41-7001.09	600	200	601	Au, Pu, U, S
9-41-7001.10	600	300	615	Au, Pu, U, S
9-41-7001.11	600	400	644	Au, S
9-41-7001.12	909	0	924	Au, Pu, Np, U, S
9-41-7001.13	900	100	902	Au, Pu, U, S
9-41-7001.14	900	200	901	Au, Pu, U, S
9-41-7001.15	900	300	915	Au, Pu, U, S
9-41-7001.16	900	400	930	Au, Pu, U, S
9-41-7001.17	900	500	960	Au, Pu, Np, U, S
9-41-7001.18	1,207	0	1,218	Au, Pu, Np, U, S
9-41-7001.19	1,200	100	1,200	Au, Pu, U, S
9-41-7001.20	1,200	200	1,200	Au, Pu, U, S
9-41-7001.21	1,200	300	1,207	Au, Pu, U, S
9-41-7001.22	1,200	400	1,222	Au, Pu, U, S
9-41-7001.23	1,200	500	1,245	Au, Pu, Np, U, S

2.1.4 Shot Priscilla. To obtain neutron flux versus ground range for this shot, a line of stations running west of ground zero was instrumented at 100-yard intervals, beginning at a distance of 300 yards from ground zero. Table 2.5 contains all data pertinent to these stations.

Project 2.3 also supported shielding studies being performed by Projects 2.4, 3.1, 3.2, and 3.3 in connection with underground structures and field fortifications.

TABLE 2.5 PROJECT 2.3 STATIONS, SHOT PRISCILLA

Station Number	Radial Distance from Ground Zero	Slant Range	Description
	yd	yd	
F-2.3-9009.03	300	380	Au, Pu, Np, U, S
F-2.3-9009.04	400	463	Au, Pu, Np, U, S
F-2.3-9009.05	500	551	Au, Pu, Np, U, S
F-2.3-9009.06	600	643	Au, Pu, Np, U, S
F-2.3-9009.07	700	737	Au, Pu, Np, U, S
F-2.3-9009.08	800	833	Au, Pu, Np, U, S
F-2.3-9009.09	900	929	Au, Pu, Np, U, S
F-2.3-9009.10	1,000	1,025	Au, Pu, Np, U, S
F-2.3-9009.11	1,100	1,124	Au, Pu, Np, U, S
F-2.3-9009.12	1,200	1,223	Au, Pu, Np, U, S

2.1.5 Shot Hood. Support was again given to the Project 2.4 shielding studies. This support was identical to that provided during Shot Franklin.

Support was given also to Project 2.10 for the measurement of neutron flux at various heights above ground. This support was identical to that given during Shot Lassen.

TABLE 2.6 PROJECT 2.3 STATIONS, SHOT OWENS

Station Number	Radial Distance from Ground Zero	Slant Range	Description
	yd	yd	
9-2.3-9004.12	100	195	Au, Pu, Np, U, S
9-2.3-9004.13	200	260	Au, Pu, Np, U, S
9-2.3-9004.14	300	343	Au, Pu, Np, U, S
9-2.3-9004.15	400	433	Au, Pu, Np, U, S
9-2.3-9004.16	500	527	Au, Pu, Np, U, S
9-2.3-9004.17	600	623	Au, Pu, Np, U, S
9-2.3-9004.18	700	720	Au, Pu, Np, U, S
9-2.3-9004.19	800	817	Au, Pu, Np, U, S
9-2.3-9004.20	900	915	Au, Pu, Np, U, S
9-2.3-9004.21	1,000	1,014	Au, Pu, Np, U, S

2.1.6 Shot Owens. Project 2.3 participation included the installation of a cable line at an azimuth of 204 degrees. Detectors were attached to this cable line at 100-yard intervals between 100 and 1,000 yards from ground zero.

Table 2.6 contains all data relative to the location of these stations.

Additional detectors were supplied to Project 2.4 for the measurement of neutron flux versus depth at varying distances from ground zero. Installation and recovery of these stations were effected by Project 2.4 personnel.

2.1.7 Shot John. Project 2.9 was supplied with sufficient detectors to instrument four locations on each of the delivery aircraft as well as two additional aircraft.

2.1.8 Shot Smoky. Project 2.3 and Project 39.5 collaborated on this shot, and three cable lines were installed along various azimuths to obtain information relative to terrain effects on neutron flux. One control line was installed south from ground zero along level terrain. The second line was installed north from ground zero over a 500-foot hill and down the back side. A third line extended northeast from ground zero over hilly terrain.

The three lines were instrumented with the usual neutron detectors supplemented by chemical dosimeters, (for integrated gamma dose measurements) germanium dosimeters, National Bureau of Standards film packs, and a group of punch-through voltage transistor dosimeters. These transistor dosimeters were used in connection with a study by the Pilotless Aircraft Division of the Boeing Airplane Company to investigate the possible future utilization of these instruments as neutron dosimeters. Additional information relative to the chemical dosimeters may be found in Reference 18.

Table 2.7 contains all information pertinent to these stations. Figure 2.2 shows a topographical view of station locations. Figures 2.3 and 2.4 show a side view of the station locations on the 58- and 353-degree lines, respectively.

2.1.9 Shot Laplace. A cable line was installed which extended from ground zero along an azimuth of 225 degrees. The detectors were attached at 100-yard intervals from ground zero at distances of 100 to 1,000 yards. Table 2.8 contains all information concerning these stations. Additional detectors were provided for Projects 2.2 and 2.4 in connection with studies of neutron induced gamma fields and neutron flux as a function of soil depth.

2.2 INSTRUMENTATION

The method used in making the neutron-flux measurements were similar to those employed during Operation Redwing (Reference 1). A list of the detectors used is given in Chapter 1. The general technique is that of neutron activation of various materials, the resultant activity being proportional to the neutron flux. Measurement of the radioactivity in the samples was accomplished at the NTS. A laboratory trailer containing all necessary counting equipment was set up near the control point for this purpose.

2.2.1 Gold Detectors. Gold was used as the thermal neutron detector. Thermal neutrons cause an (n, γ) reaction in Au^{197}, which results in the production of radioactive Au^{198}. This isotope is characterized by a 64.73 hour half life and decays to stable Hg^{198} through the emission of a 0.960 Mev beta particle followed by a 0.411 Mev gamma ray.

The cadmium-difference technique (Chapter 1) is employed, due to the cross section of gold. As shown in Figure 2.5, the gold activation cross section is essentially represented by a $1/v^2$ slope with the exception of a very-high resonance peak at approximately 5 ev. The cadmium absorption cross section, also shown in Figure 2.5, is very high in the thermal energy region but drops rapidly between 0.3 ev and 1.0 ev. This rapid change in cross section is known as the cadmium cutoff. Therefore, two gold foils were used; one shielded with cadmium, the other bare. By taking the difference in the resultant activity of the two foils, the gold resonance was eliminated, and the neutron flux below the cadmium cutoff was determined.

The gold foils were in the form of ½-inch-diameter, 10-mil thick foils. The field holders (Figure 2.6) for these foils consisted of two ¼-inch steel plates bolted together. Two cavities were milled into one of the steel plates to accept one bare and one cadmium-shielded sample. The cadmium shield was 0.045-inch thick. A mounting web was welded to one of the plates to enable the detector to be easily attached to the cable by the use of wire-rope clamps.

After irradiation, the foils were counted on scintillation counters (Section 2.2.5). Sufficient counting was accomplished to establish a decay curve for each sample. The half life was calculated from this decay curve and compared to the known half life values of Au^{198}. The counting rate at time of irradiation was determined by the following equation:

$$N_{t_0} = N_t \exp\left[+\lambda (t - t_0)\right]. \qquad (2.1)$$

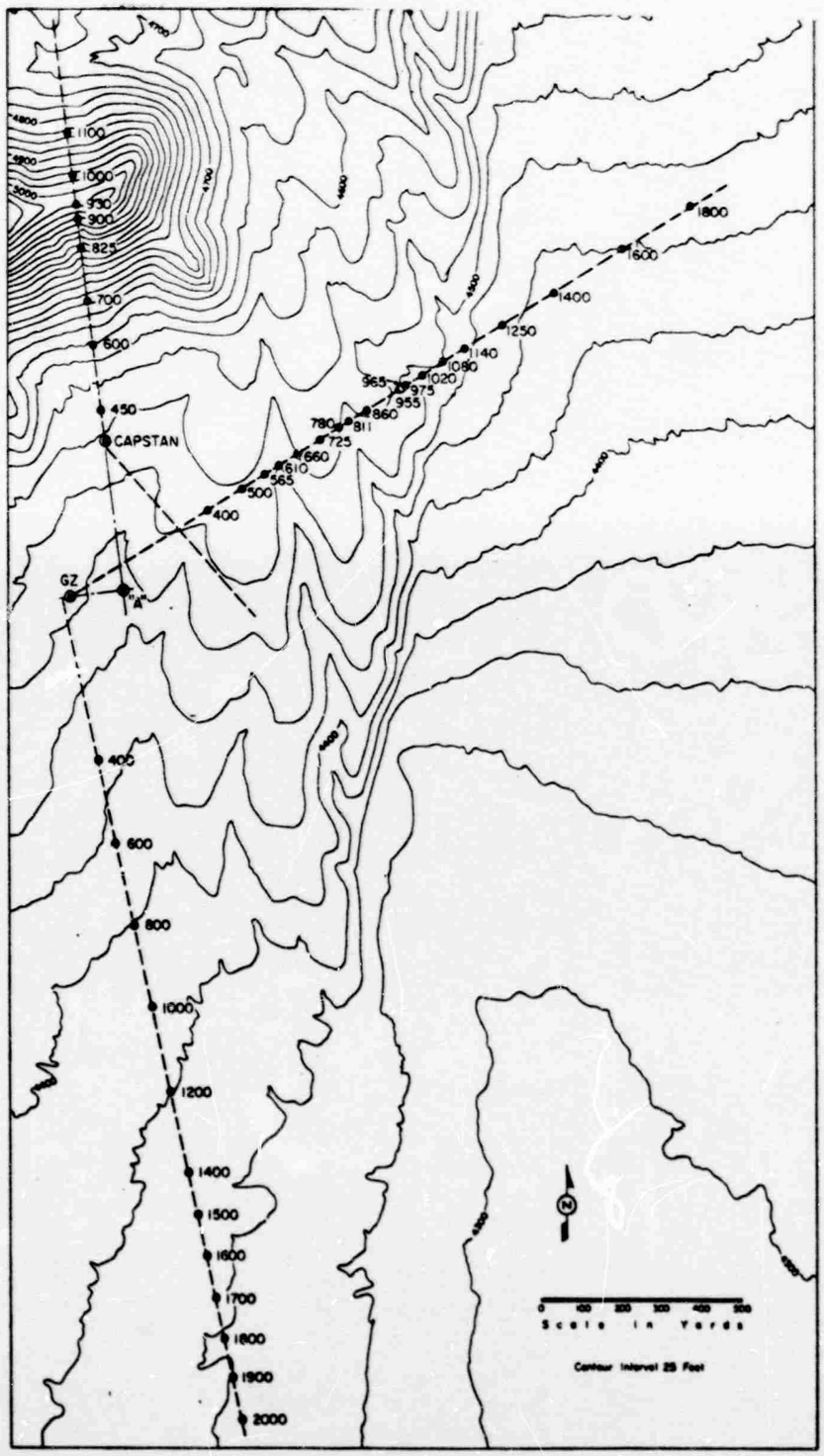

Figure 2.2 Topographical view of station locations, Shot Smoky.

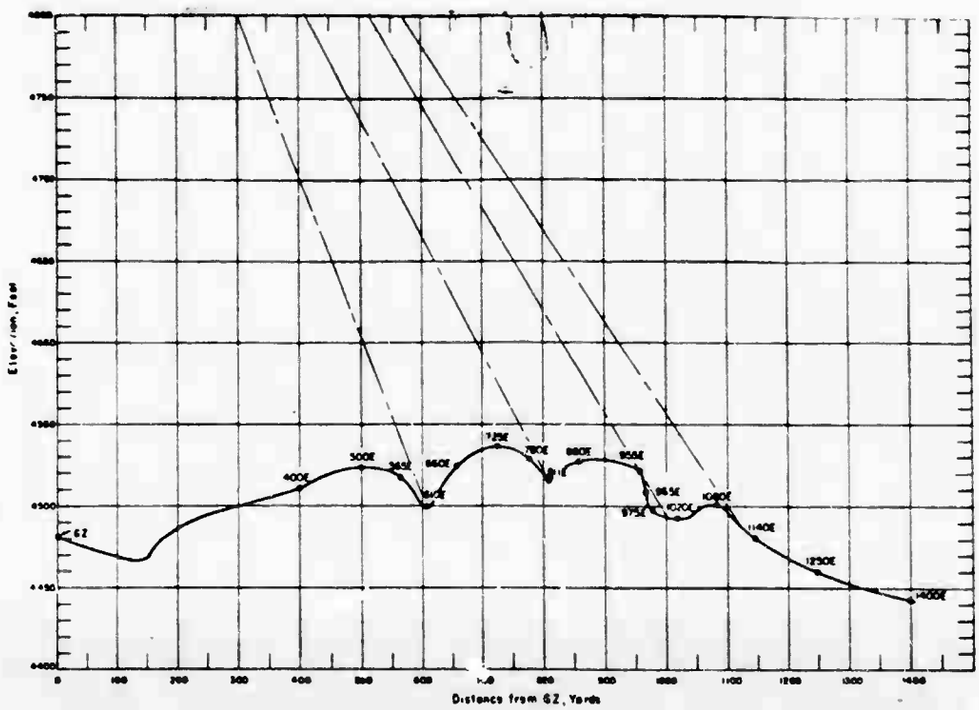

Figure 2.3 Profile of station locations on the 58-degree line, Shot Smoky.

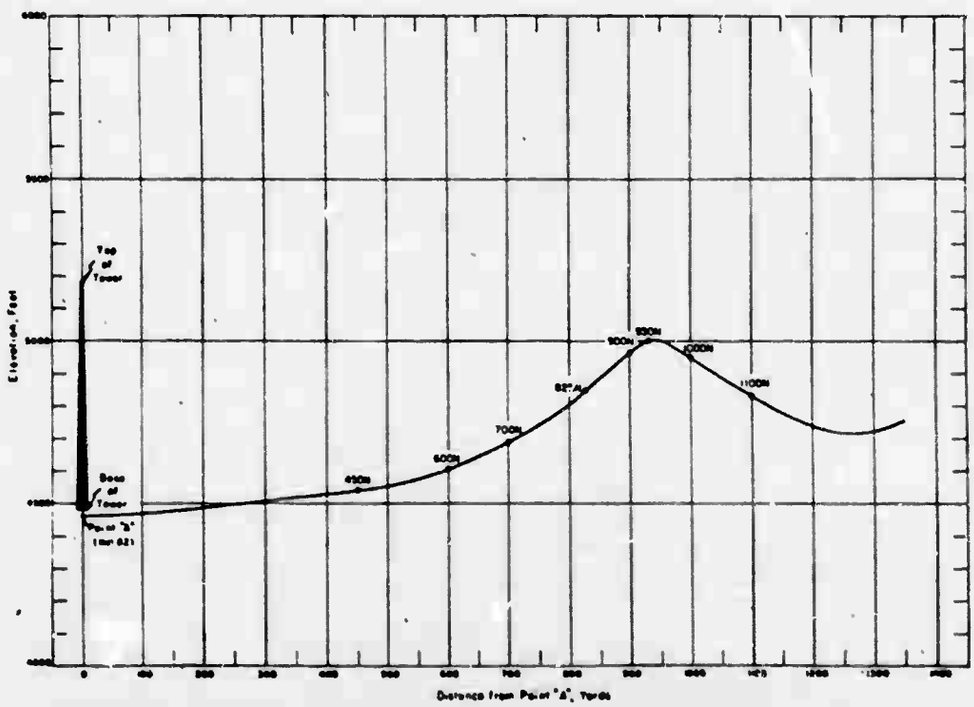

Figure 2.4 Profile of station locations on the 353-degree line, Shot Smoky. For Point A, see Figure 2.2.

TABLE 2.7 PROJECT 2.3 STATIONS, SHOT SMOKY

Station Number	Azimuth	Radial Distance from Ground Zero	Elevation with Respect to Ground Zero	Slant Range	Description	Instrumenting Agency
	deg	yd	ft	yd		
400 S	167	400	−20	466	Au, Pu, Np, S, U, NBS-F*, GD†	Project 2.3
600 S	167	600	−60	649	Au, Pu, Np, S, U, NBS-F, GD, CD‡	Project 2.3
800 S	167	800	−80	841	Au, Pu, Np, S, U, NBS-F, GD, CD	Project 2.3
1,000 S	167	1,000	−95	1,034	Au, Pu, Np, S, U, NBS-F, GD, CD	Project 2.3
1,200 S	167	1,200	−105	1,229	Au, Pu, Np, S, U, NBS-F, GD, CD	Project 2.3
1,400 S	167	1,400	−120	1,426	Au, Pu, Np, S, U, NBS-F, GD, CD	Project 2.3
1,500 S	167	1,500	−120	1,525	Au, Pu, Np, S, U, NBS-F, GD, CD	Project 39.5
1,600 S	167	1,600	−125	1,623	Au, Pu, Np, S, U, NBS-F, GD, CD	Project 39.5
1,700 S	167	1,700	−125	1,722	Au, Pu, Np, S, U, NBS-F, GD, CD	Project 39.5
1,800 S	167	1,800	−130	1,821	Au, Pu, Np, S, U, NBS-F, GD, CD	Project 39.5
1,900 S	167	1,900	−130	1,920	Au, Pu, Np, S, U, NBS-F, GD, CD	Project 39.5
2,000 S	167	2,000	−135	2,019	Au, Pu, Np, S, U, NBS-F, GD, CD	Project 39.5
450 N	353	450	+60	496	Au, Pu, Np, S, U, NBS-F, GD, CD	Project 2.3
600 N	353	600	+130	629	Au, Pu, Np, S, U, NBS-F, GD, CD	Project 2.3
700 N	353	700	+210	719	Au, Pu, Np, S, U, NBS-F, GD, CD	Project 2.3
825 N	353	825	+360	833	Au, Pu, Np, S, U, NBS-F, GD, CD	Project 2.3
900 N	353	900	+480	903	Au, Pu, Np, S, U, NBS-F, GD, CD	Project 2.3
930 N	353	930	+520	933	Au, Pu, Np, S, U, NBS-F, GD, CD	Project 2.3
1,000 N	353	1,000	+470	1,003	Au, Pu, Np, S, U, NBS-F, GD, CD	Project 39.5
1,100 N	353	1,100	+350	1,108	Au, Pu, Np, S, U, NBS-F, GD, CD	Project 39.5
400 E	58	400	+30	456	Au, Pu, Np, S, U, SB-100§	Project 2.3
500 E	58	500	+45	545	Au, Pu, Np, S, U, SB-100§	Project 2.3
565 E	58	565	+38	607	Au, Pu, Np, S, U, SB-100	Project 2.3
810 E	58	810	+21	651	Au, Pu, Np, S, U, SB-100, CD	Project 2.3
660 E	58	660	+44	891	Au, Pu, Np, S, U, SB-100, CD	Project 2.3
725 E	58	725	+56	758	Au, Pu, Np, S, U, NBS-F, GD, CD, SB-100	Project 2.3
780 E	58	780	+46	810	Au, Pu, Np, S, U, NBS-F, GD, CD, SB-100	Project 2.3
810 E	58	810	+36	841	Au, Pu, Np, S, U, NBS-F, GD, CD, SB-100	Project 2.3
860 E	58	860	+48	887	Au, Pu, Np, S, U, NBS-F, GD, CD, SB-100	Project 39.5
955 E	58	955	+41	960	Au, Pu, Np, S, U, NBS-F, GD, CD, SB-100	Project 39.5
965 E	58	965	+30	990	Au, Pu, Np, S, U, NBS-F, GD, CD	Project 39.5
975 E	58	975	+18	1,001	Au, Pu, Np, S, U, NBS-F, GD, CD	Project 39.5
1,020 E	58	1,020	+12	1,045	Au, Pu, Np, S, U, NBS-F, GD, CD, SB-100	Project 39.5
1,060 E	58	1,060	+21	1,098	Au, Pu, Np, S, U, NBS-F, GD, CD, SB-100	Project 39.5
1,140 E	58	1,140	+2	1,164	Au, Pu, Np, S, U, NBS-F, GD, CD	Project 39.5
1,250 E	58	1,250	−20	1,268	Au, Pu, Np, S, U, NBS-F, GD, CD	Project 39.5
1,400 E	58	1,400	−36	1,421	Au, Pu, Np, S, U, NBS-F, GD, CD	Project 39.5
1,600 E	58	1,600	−30	1,618	NBS-F, GD, CD	Project 39.5
1,800 E	58	1,800	−20	1,816	NBS-F, GD, CD	Project 39.5

* National Bureau of Standards film packet.
† Germanium dosimeters.
‡ Chemical dosimeters.
§ Punch-through voltage transistor dosimeter.

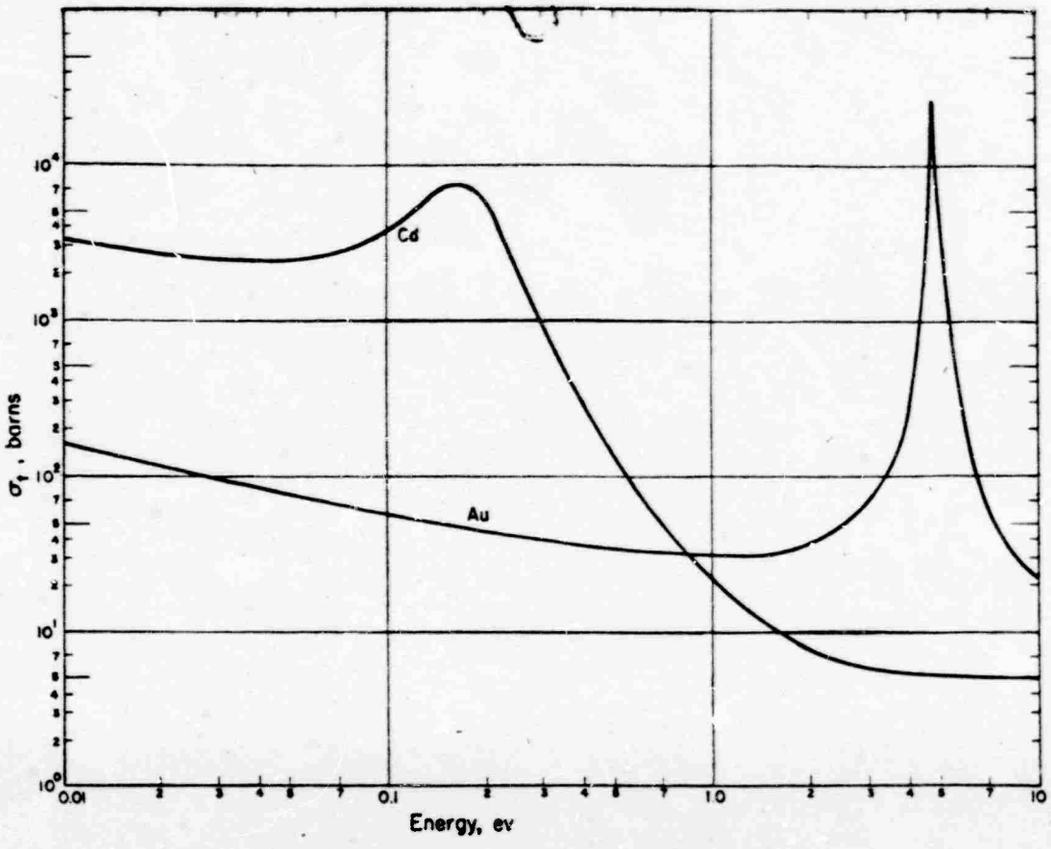

Figure 2.5 Gold and cadmium cross sections.

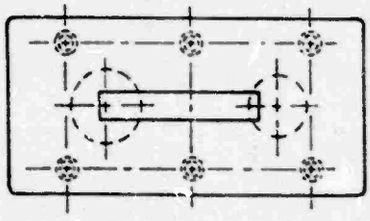

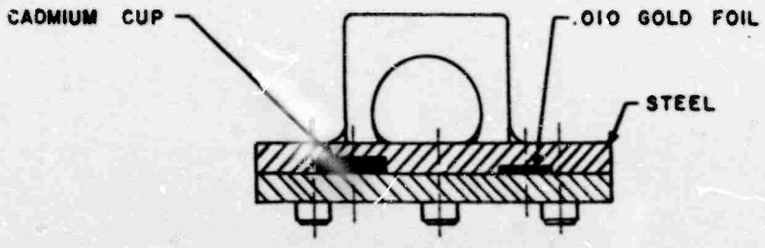

Figure 2.6 Gold-foil neutron-threshold detector.

Where: N_{t_0} = counting rate at irradiation time t_0

N_t = counting rate at time t

λ = Au^{198} decay constant

From these calculated counting rates at time t_0, the thermal neutron flux was calculated as follows:

$$F = K (N_{t_0} \text{ bare} - 1.025\ N_{t_0} \text{ shielded}) \tag{2.2}$$

Where: F = thermal neutron flux in neutrons/cm^2

K = calibration number in (neutrons/cm^2)/cpm

N_{t_0} bare = counting rate at irradiation time of unshielded sample (cpm)

N_{t_0} shielded = counting rate at irradiation time of shielded sample (cpm)

1.025 = correction number for the neutrons above the cadmium cutoff absorbed by the cadmium shield

TABLE 2.8 PROJECT 2.3 STATIONS, SHOT LAPLACE

Station Number	Radial Distance from Ground Zero	Slant Range	Description
	yd	yd	
7-2.10-9002.01	100	270	Au, Pu, Np, U, S
7-2.10-9002.02	200	324	S
7-2.10-9002.03	300	390	Au, Pu, Np, U, S
7-2.10-9002.04	400	470	S
7-2.10-9002.04A	450	510	Au, Pu, Np, U, S
7-2.10-9002.05	500	558	Au, Pu, Np, U, S
7-2.10-9002.06	600	650	S
7-2.10-9002.07	700	742	Au, Pu, Np, U, S
7-2.10-9002.08	800	837	S
7-2.10-9002.09	900	934	Au, Pu, Np, U, S
7-2.10-9002.10	1,000	1,030	S
7-2.10-9002.11	1,100	1,128	Au, Pu, Np, U, S

2.2.2 Fission Detectors. The fission detector system utilizing Pu^{239}, Np^{237}, and U^{238} was developed by G.S. Hurst, (Reference 13). These materials fission when they are bombarded with neutrons. Np^{237} and U^{238} have effective energy thresholds of 0.63 Mev and 1.5 Mev, respectively. The effective energy threshold is defined as the energy at which the fission cross section is one half of its maximum value. Pu^{239} does not have a naturally occurring energy threshold above thermal energies; however, a shield of elemental B^{10} will produce such a threshold. The effective fission cross section of Pu^{239} shielded by B^{10} is calculated, using the following expression:

$$\sigma_{eff} = \sigma_f \ e^{-\sigma_B N_B} \tag{2.3}$$

Where: σ_{eff} = effective fission cross section of Pu^{239}

σ_f = the fission cross section of Pu^{239}

σ_B = the cross section of the B^{10} (n, α) Li^7 reaction

N_B = the number of B^{10} atoms per cm^2 of surface area of the boron shield

Figure 2.7 shows the fission cross sections of the shielded fission materials. As may be seen from this figure, the effective threshold of shielded Pu^{239} is 10 kev.

The fissionable materials in the form of metal foils were sealed in thin (0.005-inch) copper dishes for ease of handling. These dishes were then placed in a cavity in a field holder (Figure 2.8) designed as a hollow steel sphere and constructed so that the periphery could be filled with B^{10}. Thus, incoming neutrons regardless of direction, must penetrate the required thickness of B^{10}. The cavity was lined with 0.025 inch of cadmium, so that any thermal neutrons produced by moderation in the shield would be captured before entering the foil.

Since these materials are naturally radioactive, a background-activity measurement was made prior to their installation in the field. After irradiation, the foils were counted using the equipment described in Section 2.2.5.

A decay curve for each sample was plotted and extrapolated to either 10 or 20 hours after irradiation (depending upon the time after detonation at which the detectors were recovered) by the superposition of the calibration decay curve (Figure 2.9). This curve for Pu^{239} fission-product activity versus time is the same for Np^{237} and U^{238} for the range of gamma energies which were measured.

The neutron flux was then determined by the following equation:

$$F = K_f N_t \tag{2.4}$$

Where: F = the neutron flux in neutrons/cm^2

K_f = the calibration number in (neutrons/cm^2)/cpm from the standard decay curve at 10 or 20 hours after irradiation for Pu^{239}, Np^{237}, and U^{238}

N_t = the counting rate in cpm of Pu^{239}, Np^{237}, or U^{238} at 10 or 20 hours after irradiation.

2.2.3 Sulfur Detectors. The reaction of interest is S^{32} (n, p) P^{32}. The resulting phosphorus-32 decays with the emission of 1.707 Mev beta particle with a 14.22 day half life. The effective threshold of this reaction is approximately 3 Mev. As can be seen in Figure 2.10, the activation cross section rises rather rapidly, beginning at an energy threshold of 1.1 Mev, and is formed by a number of relatively close resonance peaks.

The sulfur detectors were in the form of pellets which were $1\frac{1}{2}$ inches in diameter and $\frac{3}{8}$-inch thick. The pellets were formed by pouring molten sulfur into an aluminum mold and subsequently machining the pellets to the desired size. Much care was taken to produce pellets of similar weight and consistency.

The pellets, protected from shock by foam rubber, were then placed in the field holders (Figure 2.11) consisting of two aluminum plates, 4 inches long by $2\frac{1}{4}$ inches wide, which were bolted together. The top was a $\frac{1}{8}$-inch plate, while the bottom was a $\frac{5}{8}$-inch plate containing a $1\frac{5}{8}$-inch diameter hole milled to a depth of $\frac{1}{2}$ inch. Two holes were drilled at one end of the assembled plates to permit the acceptance of a $\frac{3}{4}$-inch cable clamp.

After irradiation, the resultant phosphorus-32 activity was measured by the use of techniques described in Section 2.2.5.

As in the case of the gold detectors, a decay curve was established for each sample and the half life determined. These half life determinations were then compared to the accepted half life values for P^{32}. The activity values were extrapolated to the time of irradiation by the use of Equation 2.1 where λ equaled the decay constant of P^{32}. The neutron flux was subsequently calculated by use of a calibration number.

In the case of extremely low counting rates and broken pellets, another method was used. Since the pellet is much thicker than the maximum range of the 1.72 Mev beta particles, the counting rate may be increased by removing some of the sulfur. This was done by placing all or part of the pellet in an aluminum cup and heating until the pellet melted. The sulfur was then ignited and burned off. The P^{32}, even in trace amounts, appears to form a complex with the aluminum cup and is, therefore, retained.

If the whole pellet was not burned, as was the case with broken pellets of high activity, a

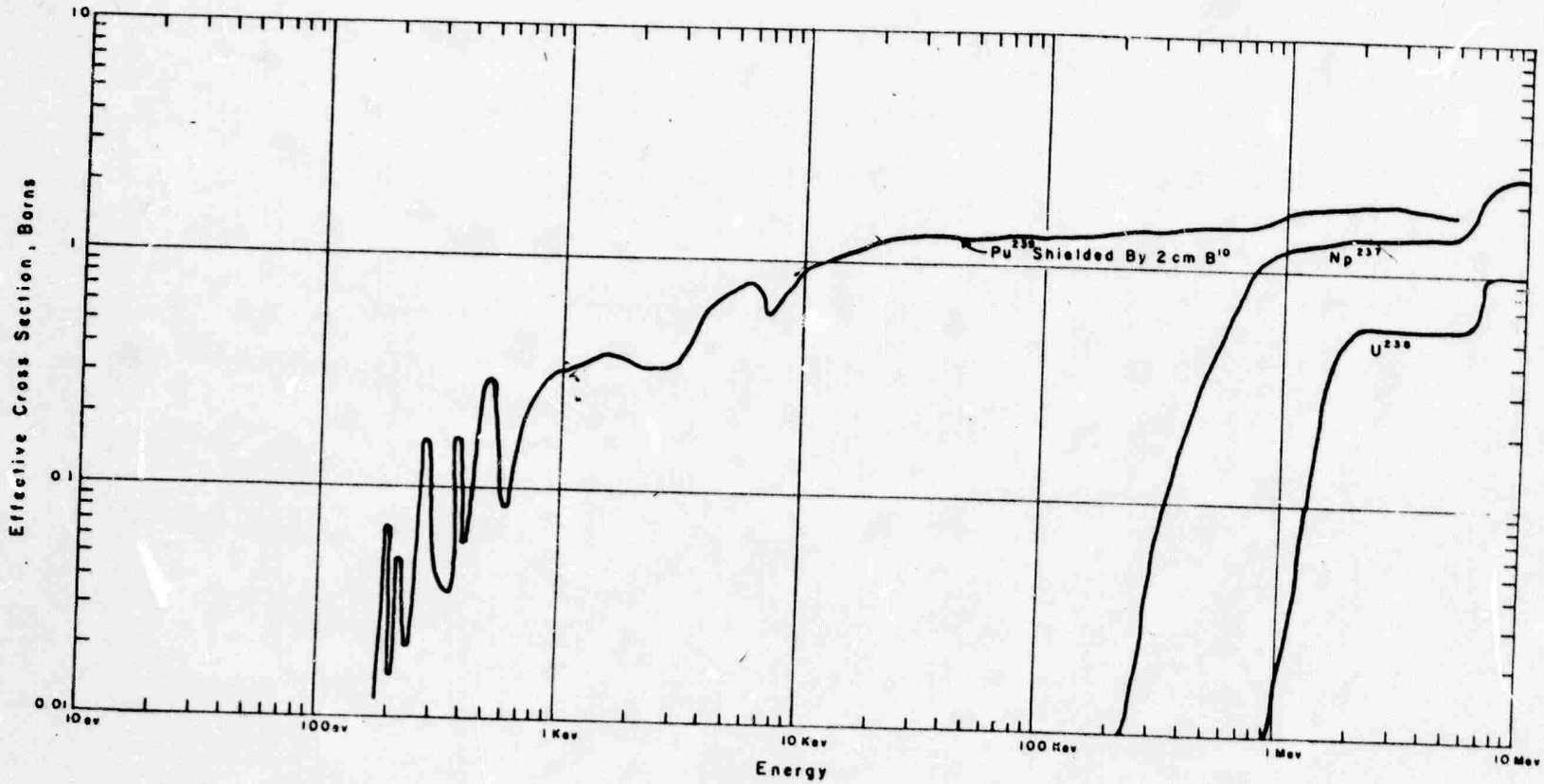

Figure 2.7 Fission-detector cross sections.

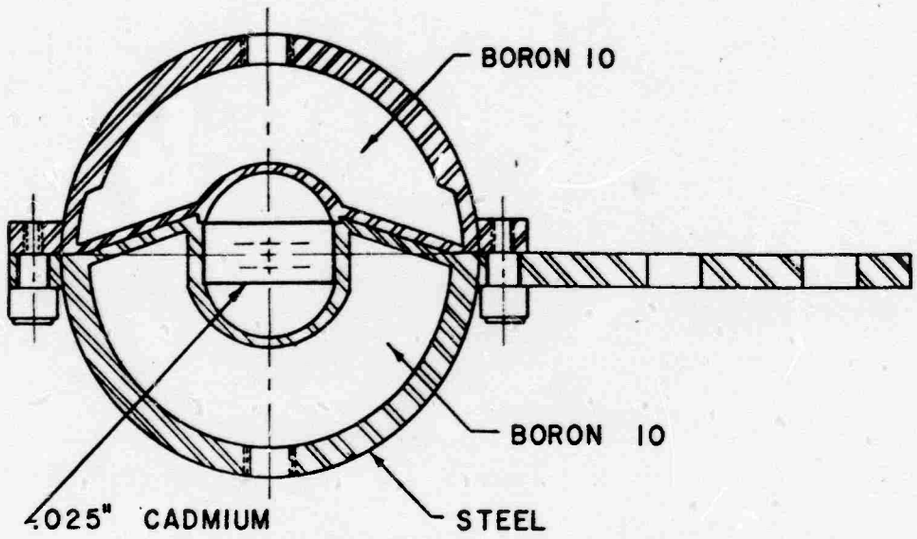

Figure 2.8 Boron-shielded neutron-threshold-detector holder.

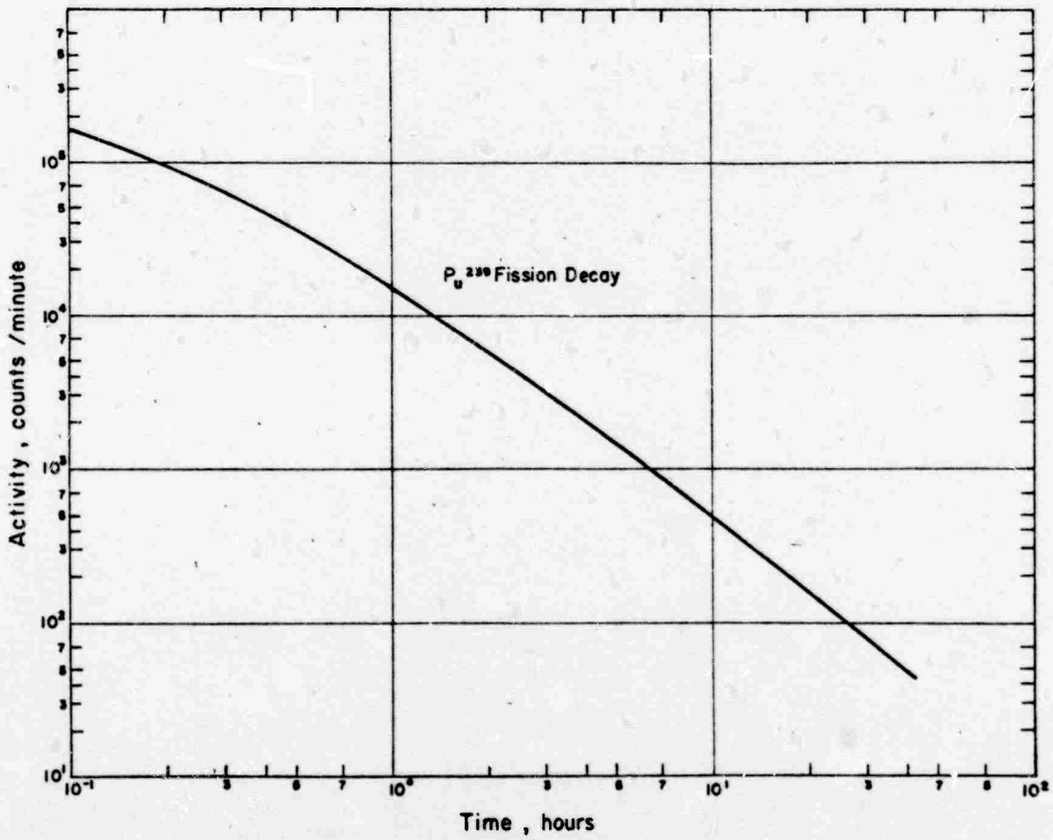

Figure 2.9 Typical fission decay curve.

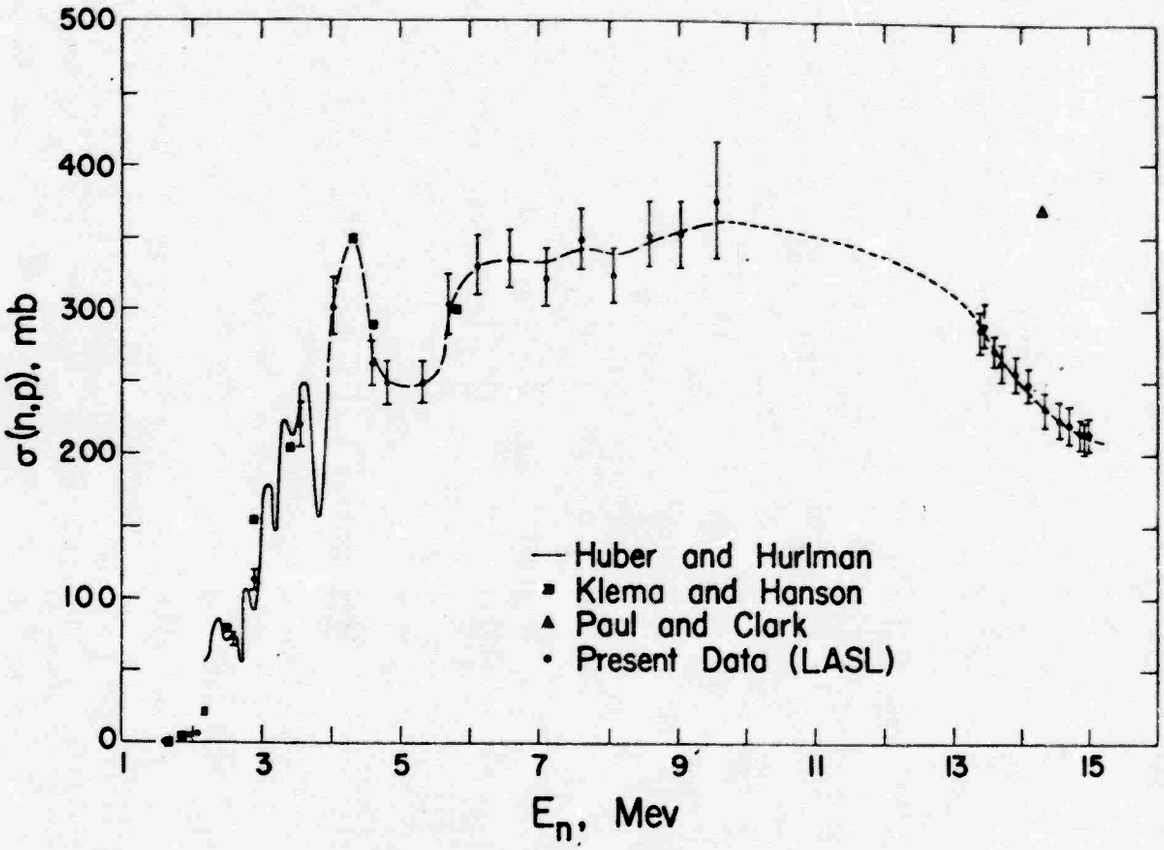

Figure 2.10 S^{32} (n, p) P^{32} cross section.

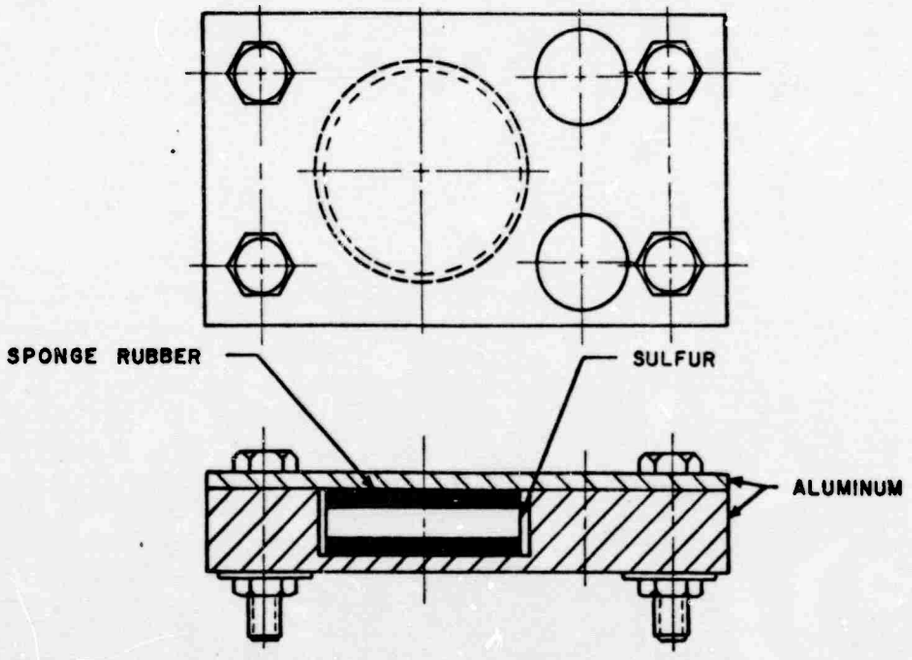

Figure 2.11 Sulfur neutron-threshold detector.

weight correction based on the weight of sulfur burned was made in the calculation of the neutron flux. This correction is represented by the following equation:

$$\text{Flux} = K_{bs} \frac{(CR_{fb})\ (Wt)}{W_{fb}} \tag{2.5}$$

Where. K_{bs} = calibration number for burned sulfur

CR_{fb} = counting rate of fraction burned

Wt = weight of whole pellet

W_{fb} = weight of fraction burned

2.2.5 Counting Equipment. Scintillation-counting techniques were used to measure the activities induced in the various detector materials. These techniques were selected such that the same equipment, with minor changes, could be used for all measurements thereby reducing the original money outlay and maintenance costs. This equipment consisted of units assembled from standard, commercially available equipment. Figure 2.13 is a block diagram of the system.

The scintillator used for gamma measurements was a 1-inch-by $1\frac{1}{2}$ inch crystal of sodium iodide. For beta activities, a Scintilon Brand plastic phosphor scintillator was used.

The gold samples were placed on a $\frac{1}{16}$-inch aluminum holder for measurement. This holder was machined to fit on the sodium iodide crystal. The electronic system was biased at approximately 300 kev which permitted good counting geometry relative to the measurement of the 411 kev gamma emitted from the Au^{198}. The electronic system was subject to some degree of instability, due to voltage drift, and therefore, was occasionally monitored with a small Co^{60} standard source.

The counting equipment used in measuring the gamma activity resulting from the (n, fission) reactions in the fission detectors was exactly the same as that used for gold. However, in this case, the bias of the discriminator was set at approximately 1.1 Mev, and the samples were mounted on a $\frac{1}{8}$-inch brass holder.

In measuring the beta particles emitted by the P^{32}, however, the plastic scintillator previously described replaced the sodium iodide crystal in the counting system. The sulfur pellets were placed directly upon the scintillator. The discriminator was set on this system just high enough to exclude photomultiplier noise. A natural uranium source was used to monitor this system.

It is necessary to measure the positron emission of Zr^{89} in the zirconium detectors due to interfering reactions. Since the direct measurement of a positron would necessitate the use of some kind of a magnetic spectrometer, it is much simpler to measure the positron-annihilation radiation. When a positron and electron annihilate, two quanta of gamma energy are emitted. The fact that they must be emitted 180 degrees apart in order to conserve momentum makes this measurement not only possible but easily accomplished. Two sodium iodide crystals and photomultiplier units of the type used in the counting of the gold and fission samples were assembled

with the crystals facing each other. The irradiated zirconium samples were then placed in an aluminum holder between the crystals, and the output of the two tubes was fed into a coincidence circuit. In order to reduce accidental coincidences due to high backgrounds and other activities, the amplifier associated with each photomultiplier assembly was designed in a manner that allowed the setting of an energy window. This window was set between 400 kev and 600 kev. Na^{22}, which is also a positron emitter, was used as the monitoring source for this system.

All the monitoring sources were selected due to their long half lives, which minimized decay corrections.

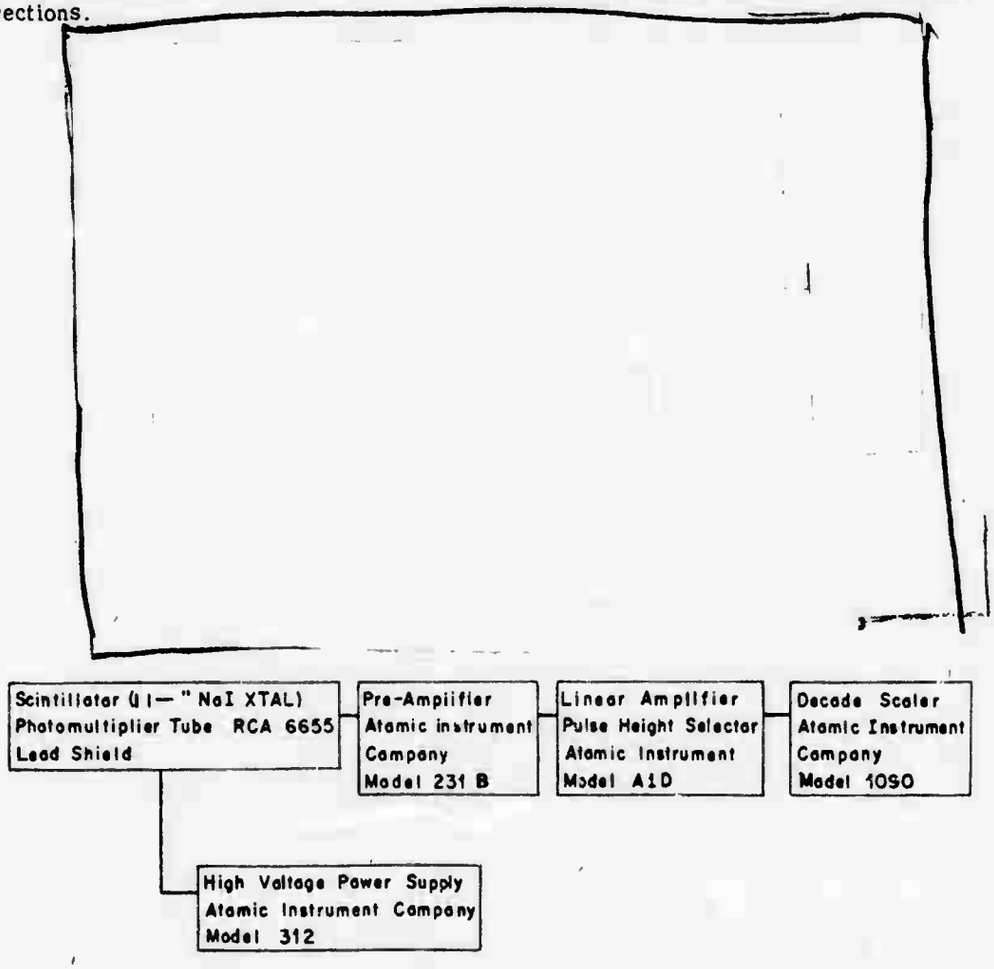

Figure 2.13 Block diagram of counting equipment.

2.2.6 Calibration. Calibration of the detectors was accomplished utilizing the facilities at LASL during the period from 1 April to 10 April 1959. Additional calibrations were performed in the spring and fall of 1958 (Reference 19).

2.2.7 Gold-Detector Calibration. Calibration of the gold detectors was accomplished by irradiation of the gold samples in the south thermal column of the Omega water boiler at LASL. The procedure for determining the counting rate at the time of irradiation was the same as that described in Section 2.2.1. During the first calibration run, two separate determinations were made. The total flux on the first run was 1.5×10^{10} neutrons/cm^2, while that for the second run was 3.15×10^{10} neutrons/cm^2. The counting rate at time of irradiation was 2.50×10^4 counts/min and 5.40×10^4 counts/min, respectively, for the two runs. Calibration numbers were calculated to be 5.00×10^5 (neutrons/cm^2)/(count/min) and 5.83×10^5 (neutrons/cm^2)/(count/min), respec-

tively. As has been mentioned in Section 2.2.6, additional calibrations which yielded similar results were accomplished in the spring and fall of 1958. Thermal calibrations which were performed in this period of time along with the two mentioned above have been averaged, and the resulting calibration number of $6.07 \times 10^5 \pm 10$ percent (neutrons/cm^2)/(count/min) has been used in all calculations associated with the neutron flux measured by the use of gold foils during Operation Plumbbob.

2.2.8 Fission-Detector Calibration. Calibration of the fission detector system was accomplished at LASL. Samples were exposed to the thermal flux of both the north and south thermal columns of the Omega water boiler.

The plutonium samples used for calibration purposes were unshielded metal disks, 1 mil thick and ½ inch in diameter and weighing 47 mg each. The sample was kept as small as possible, in order to minimize both the absorption of the thermal neutrons in the sample itself and the flux depression caused by the placing of a material of high cross section in a thermal-neutron-flux field.

A correction for self-absorption and flux depression for the sample in question was determined experimentally by LASL personnel by the exposure of plutonium samples of various weights to the thermal neutron flux and extrapolating to zero weight. The correction for the sample size used was found to be 1.18. During the original calibration, the samples were exposed to thermal fluxes of 1.76×10^{10} neutrons/cm^2 and 3.30×10^{10} neutrons/cm^2. The flux at point of insertion in the reaction was calculated on the basis of power and quoted as accurate to ± 10 percent.

The samples were counted as described in Section 2.2.5. The counting rate at 10 and 20 hours was determined by use of the plotted decay of each sample. Calibration numbers for all fission samples (plutonium, neptunium, and uranium) were calculated as follows:

$$K_{\text{fission}} = \frac{\text{Flux}}{(1.18)\ \dfrac{\text{counting rate}}{\text{weight}}\ \dfrac{\text{fast cross section of } Pu^{239},\ Np^{237},\ \text{or } U^{238}}{\text{thermal cross section of } Pu^{239}}} \qquad (2.6)$$

The thermal-neutron-fission-cross-section values used for plutonium was 746 barns; the fast-neutron-fission-cross-section values were 1.83 barns, 1.4 barns, and 0.55 barn for plutonium, neptunium and uranium, respectively. The calculated calibration numbers at 10 hours were:

$K_{Pu^{239}} = 2.10 \times 10^8$ (neutrons/cm^2)/(cpm/gram)

$K_{Np^{237}} = 2.62 \times 10^8$ (neutrons/cm^2)/(cpm/gram)

$K_{U^{238}} = 6.66 \times 10^6$ (neutrons/cm^2)/(cpm/gram)

At 20 hours, the calculated calibration numbers were:

$K_{Pu^{239}} = 7.51 \times 10^8$ (neutrons/cm^2)/(cpm/gram)

$K_{Np^{237}} = 9.82 \times 10^8$ (neutrons/cm^2)/(cpm/gram)

$K_{U^{238}} = 2.33 \times 10^9$ (neutrons/cm^2)/(cpm/gram)

Additional calibrations of fission detectors which were preformed at LASL after the completion of the field phase of Operation Plumbbob yielded results which were similar to those mentioned above. Results were averaged for each type of detector and the resulting figures were used in the calculation of the data presented in this report. These average calibration numbers at 10 hours are:

$K_{Pu^{239}} = 2.21 \times 10^8 \pm 10$ percent (neutrons/cm^2)/(cpm/gram)

$K_{Np^{237}} = 2.89 \times 10^8 \pm 10$ percent (neutrons/cm^2)/(cpm/gram)

$K_{U^{238}} = 7.35 \times 10^8 \pm 10$ percent (neutrons/cm^2)/(cpm/gram)

At 20 hours the average calibration numbers are:

$K_{Pu^{239}} = 7.75 \times 10^8 \pm 10$ percent (neutrons/cm^2)/(cpm/gram)

$K_{Np^{237}} = 1.01 \times 10^9 \pm 10$ percent (neutrons/cm^2)/(cpm/gram)

$K_{U^{238}} = 2.58 \times 10^9 \pm 10$ percent (neutrons/cm^2)/(cpm/gram)

2.2.9 Sulfur Detector Calibration. The Cockroft-Walton accelerator at LASL was used to calibrate the sulfur pellets. Targets consisted of zirconium foils impregnated with tritium. The Cockroft-Walton ion source was rf ionized deuterium. The energy of the accelerated deuterons was 250 kev. The reaction used for the production of 14.2 Mev neutrons was as follows:

$$1D^2 + 1T^3 = 2He^4 + 0n^1 + Q$$

The number of neutrons produced in the target was measured by the monitoring of the number of alpha particles emitted.

The samples were exposed to total fluxes of 6.68×10^{10} neutrons/cm^2 and 5.83×10^{10} neutrons/cm^2 in their field holders. These fluxes were accumulated during several 10-minute exposures, spread over a time of approximately 6 hours. This prodecure gave a reasonable counting rate in the sulfur. Since the time of irradiation was short, in comparison to the half life of the P^{32} formed, no correction was made for decay during irradiation. Calculation of the resultant activity at the time of irradiation was the same as that described in Section 2.2.3. Several determinations were made, and the average calibration number was found to be 1.10×10^7 (neutrons/cm^2)/(count/min). It can be seen from Figure 2.10 that the cross section for the (n, p) reaction at 14 Mev is approximately 250 millibarns. This should give a calibration for the flux in the lower energy regions of the sulfur detector's range. The average activation cross section between 3 Mev and 7 Mev is apparently 250 millibarns while between 7 and 13 the average will be about 300 millibarns. Since the percentage of neutrons from the fission process in the region between 7 and 13 Mev is small, it is felt that the calibration using 14-Mev neutrons does not introduce any appreciable error in either the flux or dose measurements made using sulfur as a detector. Additionally, ten more sulfur calibrations have been performed since the completion of the field phase of Operation Plumbbob. The results of these additional calibrations, along with those previously mentioned, have been averaged and the resulting figure of $1.06 \times 10^7 \pm 10$ percent (neutrons/cm^2)/(count/min) has been used in calibrating the sulfur fluxes reported in the following chapter.

Chapter 3
RESULTS

3.1 NEUTRON FLUX

3.1.1 Shot Franklin. Results of the neutron flux measurements from Shot Franklin are summarized in Table 3.1. Due to the low neutron flux encountered, some of the activated samples contained quantities of radioactivity too small to be measured. This was especially true in the case of the neptunium and uranium detectors. Figure 3.1 is a representation of neutron flux times slant range squared versus slant range. The straight lines are drawn parallel through the points, since previous measurements have shown that the neutron spectrum for neutron energies above the thermal range does not change with distance from ground zero (Reference 1). In drawing parallel lines through the data, the correctness of this previous finding has been assumed and is referred to as the parallel line assumption.

The results obtained in connection with the Project 2.4 tank armor shielding studies are omitted, since the data itself without an explanation of exposure conditions would be of little value. This data and its interpretation is fully presented in ITR – 1413 (Reference 20).

3.1.2 Shct Lassen. The results of the neutron flux measurements from Shot Lassen are included in Table 3.2. Due to the unexpected low yield of about 0.47 tons, data from all but the gold detectors was very limited. Figure 3.2 is a representation of flux versus slant range. Data obtained from the Project 2.4 tank-shielding studies have been omitted, since these results and their explanations are covered completely in the report of Project 2.4. No data was obtained in support of Project 2.10, relative to their measurement of neutron flux at various heights above the ground, because of the low yield.

3.1.3 Shot Wilson. The results of the neutron flux measurements from the Project 2.4 shielding-studies are given in ITR–1413.

Results obtained in connection with the Project 41.3 measurements of neutron flux versus height above the ground are found in Table 3.3. Since measurements taken at stations along the ground were directly applicable to the flux-versus-slant-range measurements, the data were handled accordingly and are plotted in Figure 3.3.

3.1.4 Shot Priscilla. Results of the neutron flux measurements from Shot Priscilla are presented in Table 3.4. Figure 3.4 is a representation of these measurements in which the parallel-line assumption is applicable. It should be noted, however, that the data from the three stations nearest ground zero do not fit this assumption.

The results from the detectors utilized for the shielding studies conducted by Project 2.4 on tanks, underground structures, and field fortifications can be found in ITR–1413.

3.1.5 Shot Hood. Results of the neutron flux measurements from Shot Hood in connection with the Project 2.4 shielding studies are presented in ITR–1413. The neutron flux measurements made in conjunction with the Project 2.10 studies of neutron flux at various heights above ground can be found in ITR–1419.

3.1.6 Shot Owens. Results of the neutron flux measurements made at Shot Owens are given in Table 3.5. Figure 3.5 is a representation of flux versus slant range.

Neutron flux measurements made during the Project 2.4 study of flux versus depth are summarized in Table 3.6. Neutron flux variation with depth has been the subject of discussion and

TABLE 3.1 RESULTS OF NEUTRON-THRESHOLD-DETECTOR MEASUREMENTS, SHOT FRANKLIN

Station Number	Slant Range	Measured Flux			
		Au	Pu	Np	U
	yds	n/cm^2	n/cm^2	n/cm^2	n/cm^2
3-2.3-9001.01	158	7.89×10^{12}	1.21×10^{13}	7.40×10^{12}	1.75×10^{12}
3-2.3-9001.02	218	4.41×10^{12}	6.10×10^{12}	4.17×10^{12}	9.50×10^{11}
3-2.3-9001.03	327	9.65×10^{11}	1.84×10^{12}	9.68×10^{11}	2.80×10^{11}
3-2.3-9001.04	437	2.70×10^{11}	7.17×10^{11}	4.00×10^{11}	1.02×10^{11}
3-2.3-9001.05	547	9.23×10^{10}	2.77×10^{11}	2.25×10^{11}	5.49×10^{10}
3-2.3-9001.06	656	4.20×10^{10}	1.43×10^{11}	—	2.79×10^{10}
3-2.3-9001.07	766	1.99×10^{10}	7.61×10^{10}	—	—
3-2.3-9001.08	876	9.83×10^{9}	3.22×10^{10}	—	—
3-2.3-9001.09	985	5.43×10^{9}	1.72×10^{10}	—	—
3-2.3-9001.10	1,094	2.76×10^{9}	—	—	—

analysis in ITR-1410, ITR-1411 (Reference 22), and ITR-1413. Measurements obtained during the Project 2.10 studies of flux versus altitude are found in ITR-1419.

3.1.7 Shot John. No results were obtained from this shot due to the apparently low neutron flux which occurred at the aircraft positions. This fact in itself was useful, since it indicated the upper limit of possible neutron dose to the aircrews involved. ITR-1418 (Reference 23) contains a discussion of this subject.

TABLE 3.2 RESULTS OF NEUTRON-THRESHOLD-DETECTOR MEASUREMENTS, SHOT LASSEN

Station Number	Slant Range	Measured Flux			
		Au	Pu	Np	U
	yds	n/cm^2	n/cm^2	n/cm^2	n/cm^2
9-2.3-9004.01	195	1.52×10^{10}	5.13×10^{10}	1.89×10^{10}	9.58×10^{9}
9-2.3-9004.02	260	8.07×10^{9}	3.95×10^{10}	—	7.28×10^{9}
9-2.3-9004.03	343	4.24×10^{9}	1.96×10^{10}	—	—
9-2.3-9004.04	433	1.83×10^{9}	9.70×10^{9}	—	—
9-2.3-9004.05	527	1.10×10^{9}	—	—	—
9-2.3-9004.06	623	4.67×10^{8}	—	—	—
9-2.3-9004.07	720	2.74×10^{8}	—	—	—
9-2.3-9004.08	817	1.51×10^{8}	—	—	—
9-2.3-9004.09	915	7.77×10^{7}	—	—	—
9-2.3-9004.10	1,014	4.42×10^{7}	—	—	—

3.1.8 Shot Smoky. Results from Shot Smoky are found in Table 3.7. Figures 3.6, 3.7, and 3.8 show plots of flux versus slant range.

Because of the high fallout contamination, it was impossible to recover some of the detectors until H + 72 hours. Even at this late time, gamma decays were taken for each sample. These decay curves were extrapolated to H + 20 hours by superposition of the calibration decay curve. The curve used for this purpose was a composite curve taken from several samples which were

Text continued on Page 43.

TABLE 3.3 PROJECT 41.3, SHOT WILSON

Station Number	Radial Distance from Ground Zero	Height Above Ground	Measured Flux			
			Au	Pu	Np	U
	yd	ft	n/cm²	n/cm²	n/cm²	n/cm²
9-41-7001.01	0	0	6.58×10^{14}	—	—	—
9-41-7001.01F	200	0	—	1.92×10^{14}	—	1.68×10^{14}
9-41-7001.02	100	350	*	—	—	—
9-41-7001.03	317	0	9.41×10^{12}	1.91×10^{14}	9.90×10^{12}	1.87×10^{13}
9-41-7001.04	300	233	1.08×10^{14}	—	—	—
9-41-7001.05	300	487	1.22×10^{14}	—	—	—
9-41-7001.06	300	700	8.55×10^{13}	—	—	—
9-41-7001.07	577	0	1.10×10^{12}	2.77×10^{12}	1.71×10^{12}	3.82×10^{13}
9-41-7001.08	600	300	5.33×10^{12}	1.48×10^{12}	—	3.09×10^{13}
9-41-7001.09	600	800	5.97×10^{12}	3.12×10^{13}	—	1.93×10^{13}
9-41-7001.10	600	900	6.44×10^{12}	4.19×10^{13}	—	5.09×10^{12}
9-41-7001.11	600	1,200	8.50×10^{12}	2.77×10^{13}	2.39×10^{13}	3.87×10^{12}
9-41-7001.12	909	0	6.47×10^{11}	3.25×10^{13}	1.82×10^{12}	5.26×10^{11}
9-41-7001.13	900	300	5.48×10^{11}	4.60×10^{13}	—	7.24×10^{11}
9-41-7001.14	900	600	8.87×10^{11}	4.01×10^{13}	—	7.37×10^{11}
9-41-7001.15	900	900	8.81×10^{11}	7.02×10^{12}	—	8.73×10^{11}
9-41-7001.16	900	1,200	6.87×10^{11}	6.37×10^{12}	—	8.38×10^{11}
9-41-7001.17	900	1,500	2.49×10^{13}	5.52×10^{13}	3.42×10^{13}	7.49×10^{11}
9-41-7001.18	1,207	0	2.00×10^{11}	5.55×10^{11}	3.18×10^{11}	1.18×10^{11}
9-41-7001.19	1,200	300	1.28×10^{11}	9.35×10^{11}	—	1.40×10^{11}
9-41-7001.20	1,200	600	1.19×10^{11}	1.09×10^{13}	—	1.77×10^{11}
9-41-7001.21	1,200	900	1.33×10^{11}	1.21×10^{12}	—	1.71×10^{11}
9-41-7001.22	1,200	1,200	1.97×10^{11}	1.22×10^{12}	—	1.70×10^{11}
9-41-7001.23	1,200	1,500	8.88×10^{10}	1.07×10^{12}	6.78×10^{11}	1.88×10^{11}

* Samples were not recovered.

TABLE 3.4 RESULTS OF NEUTRON-THRESHOLD-DETECTOR MEASUREMENTS, SHOT PRISCILLA

Station Number	Slant Range	Measured Flux			
		Au	Pu	Np	U
	yds	n/cm²	n/cm²	n/cm²	n/cm²
F-2.3-9009.03	380	—	5.94×10^{14}	1.85×10^{14}	6.33×10^{13}
F-2.3-9009.04	463	8.44×10^{13}	1.47×10^{14}	9.08×10^{13}	3.39×10^{13}
F-2.3-9009.05	552	3.83×10^{13}	1.32×10^{14}	4.56×10^{13}	1.68×10^{13}
F-2.3-9009.06	644	5.29×10^{12}	1.82×10^{13}	1.28×10^{13}	3.30×10^{12}
F-2.3-9009.07	738	2.83×10^{13}	1.05×10^{13}	8.13×10^{12}	1.77×10^{13}
F-2.3-9009.08	833	1.88×10^{13}	6.02×10^{13}	3.49×10^{13}	1.05×10^{13}
F-2.3-9009.09	930	8.73×10^{11}	2.89×10^{13}	1.81×10^{13}	5.93×10^{11}
F-2.3-9009.10	1,027	5.08×10^{11}	1.75×10^{13}	1.12×10^{13}	2.94×10^{11}
F-2.3-9009.11	1,124	3.20×10^{11}	9.97×10^{11}	5.05×10^{11}	1.88×10^{11}
F-2.3-9009.12	1,222	1.71×10^{11}	5.35×10^{11}	2.68×10^{11}	1.18×10^{11}

TABLE 3.5 RESULTS OF NEUTRON-THRESHOLD-DETECTOR MEASUREMENTS, SHOT OWENS

Station Number	Slant Range	Measured Flux			
		Au	Pu	Np	U
	yds	n/cm²	n/cm²	n/cm²	n/cm²
9-2.3-9004.12	195	3.77×10^{14}	2.23×10^{15}	9.82×10^{14}	2.54×10^{14}
9-2.3-9004.13	280	1.98×10^{14}	1.17×10^{15}	7.64×10^{14}	1.45×10^{14}
9-2.3-9004.14	343	1.21×10^{14}	4.72×10^{14}	2.48×10^{14}	8.04×10^{12}
9-2.3-9004.15	433	4.87×10^{12}	2.43×10^{14}	9.51×10^{13}	4.38×10^{12}
9-2.3-9004.18	527	2.71×10^{12}	9.82×10^{13}	5.71×10^{13}	1.24×10^{13}
9-2.3-9004.17	823	1.33×10^{12}	6.10×10^{12}	4.50×10^{12}	1.04×10^{13}
9-2.3-9004.18	720	6.49×10^{12}	4.19×10^{12}	2.82×10^{13}	5.79×10^{13}
9-2.3-9004.19	817	3.81×10^{13}	1.47×10^{13}	1.97×10^{12}	2.33×10^{12}
9-2.3-9004.20	915	1.50×10^{12}	7.65×10^{12}	—	1.54×10^{12}
9-2.3-9004.21	1,014	9.35×10^{11}	5.10×10^{13}	—	7.95×10^{11}

TABLE 3.6 PROJECT 2.4 DEPTH MEASUREMENTS, SHOT OWENS

Distance from Ground Zero	Depth	Gold Flux	Plutonium Flux	Uranium Flux
yds	cm	n/cm^3	n/cm^3	n/cm^3
200	0	2.11×10^{14}	—	—
	15	3.88×10^{14}	2.64×10^{14}	4.43×10^{13}
	30	1.13×10^{13}	4.05×10^{13}	2.39×10^{13}
	45	5.22×10^{13}	3.67×10^{13}	8.73×10^{12}
	60	1.93×10^{13}	1.22×10^{13}	4.84×10^{13}
	75	4.46×10^{13}	3.67×10^{11}	1.62×10^{13}
	90	1.11×10^{12}	1.74×10^{13}	5.61×10^{11}
300	0	9.52×10^{13}	—	—
	15	1.05×10^{14}	2.20×10^{14}	3.90×10^{13}
	30	5.64×10^{13}	5.00×10^{13}	7.15×10^{13}
	45	1.77×10^{13}	9.70×10^{12}	3.22×10^{12}
	60	4.47×10^{12}	3.78×10^{12}	1.39×10^{12}
	75	8.92×10^{11}	1.48×10^{13}	5.87×10^{11}
	90	7.77×10^{11}	5.18×10^{11}	2.33×10^{11}
400	0	4.63×10^{13}	—	—
	15	6.86×10^{13}	8.62×10^{13}	9.62×10^{13}
	30	2.79×10^{13}	1.22×10^{13}	3.45×10^{13}
	45	9.95×10^{12}	3.94×10^{12}	1.36×10^{11}
	80	1.89×10^{13}	1.47×10^{12}	4.62×10^{11}
	75	7.22×10^{11}	3.78×10^{11}	1.48×10^{11}
	90	2.15×10^{11}	2.26×10^{11}	9.73×10^{10}

TABLE 3.7 NEUTRON-THRESHOLD-DETECTOR MEASUREMENTS, SHOT SMOKY

Station Number	Distance from Ground Zero	Slant Range	Measured Flux			
			Au	Pu	Np	U
	yds	yds	n/cm^3	n/cm^3	n/cm^3	n/cm^3
400 S	400	466	2.18×10^{13}	7.46×10^{13}	4.99×10^{13}	—
600 S	600	649	—	2.18×10^{13}	1.22×10^{13}	1.95×10^{13}
800 S	800	841	1.59×10^{13}	5.90×10^{13}	—	5.52×10^{11}
1,000 S	1,000	1,034	4.85×10^{11}	2.31×10^{13}	—	1.11×10^{11}
1,200 S	1,200	1,229	1.69×10^{11}	7.14×10^{11}	—	—
1,400 S	1,400	1,428	—	8.07×10^{11}	—	—
450 N	450	498	4.75×10^{13}	8.23×10^{13}	6.74×10^{13}	9.26×10^{13}
600 N	600	629	1.54×10^{13}	4.08×10^{13}	3.35×10^{13}	4.85×10^{13}
700 N	700	719	6.80×10^{13}	2.23×10^{13}	1.68×10^{13}	2.95×10^{13}
825 N	825	833	1.67×10^{13}	1.31×10^{13}	9.89×10^{13}	1.47×10^{13}
900 N	900	903	2.13×10^{13}	9.37×10^{13}	—	8.53×10^{11}
930 N	930	933	1.64×10^{13}	—	—	6.31×10^{11}
400 E	400	458	6.73×10^{13}	9.90×10^{13}	8.87×10^{13}	1.72×10^{13}
500 E	500	545	2.38×10^{13}	4.79×10^{13}	4.16×10^{13}	6.16×10^{13}
565 E	565	607	1.42×10^{13}	4.06×10^{13}	3.60×10^{13}	4.91×10^{13}
605 E	605	651	6.31×10^{13}	2.96×10^{13}	2.51×10^{13}	3.62×10^{12}
660 E	660	691	6.25×10^{13}	2.03×10^{13}	1.46×10^{13}	2.79×10^{12}
725 E	725	758	3.69×10^{13}	1.31×10^{13}	6.88×10^{13}	1.72×10^{13}
780 E	780	810	2.75×10^{13}	9.64×10^{13}	8.26×10^{13}	1.19×10^{13}
610 E	610	841	—	7.41×10^{12}	6.92×10^{13}	9.84×10^{11}

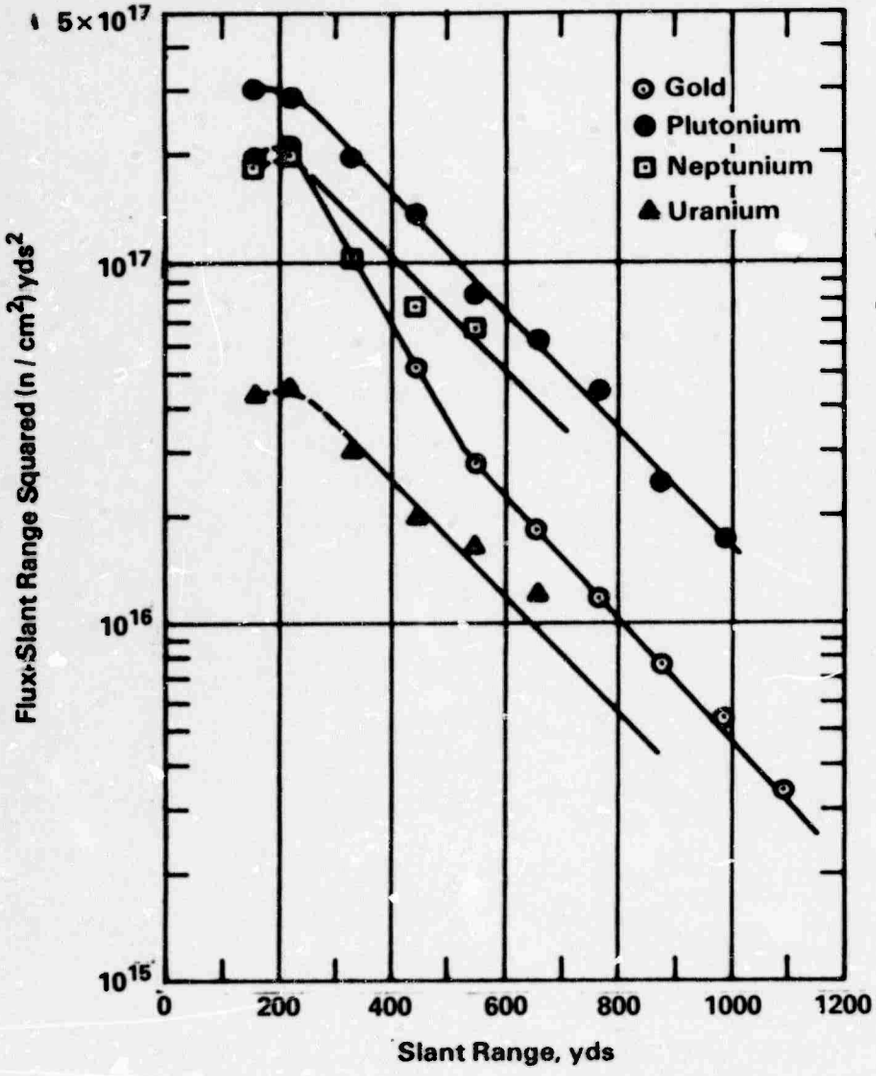

Figure 3.1 Neutron-Threshold-Detector Results, Shot Franklin.

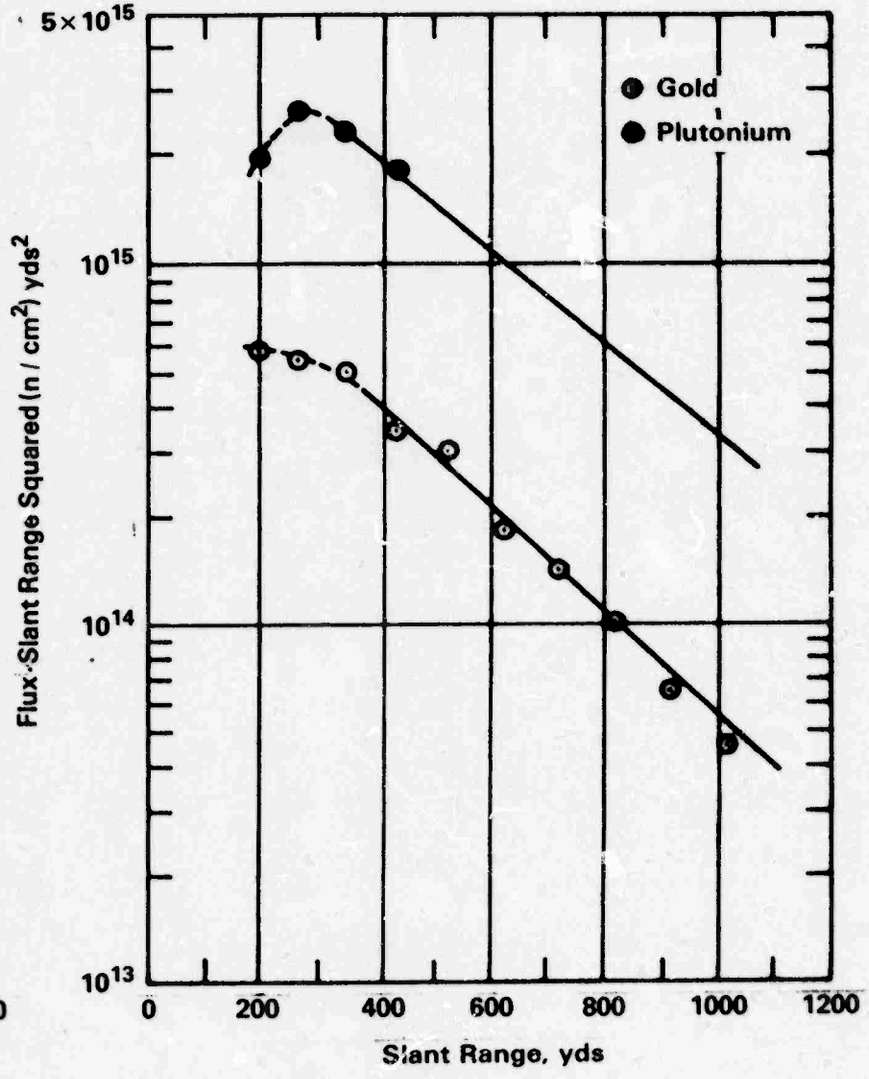

Figure 3.2 Neutron-Threshold-Detector Results, Shot Lassen.

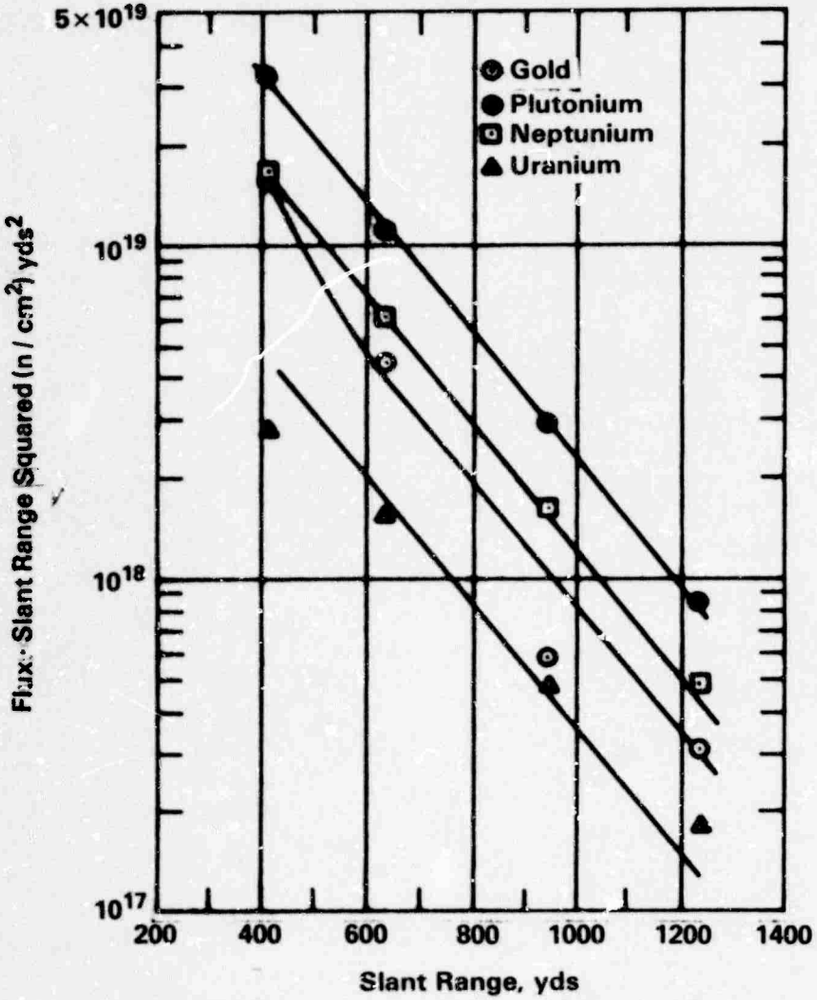

Figure 3.3 Neutron-Threshold-Detector Results, Shot Wilson.

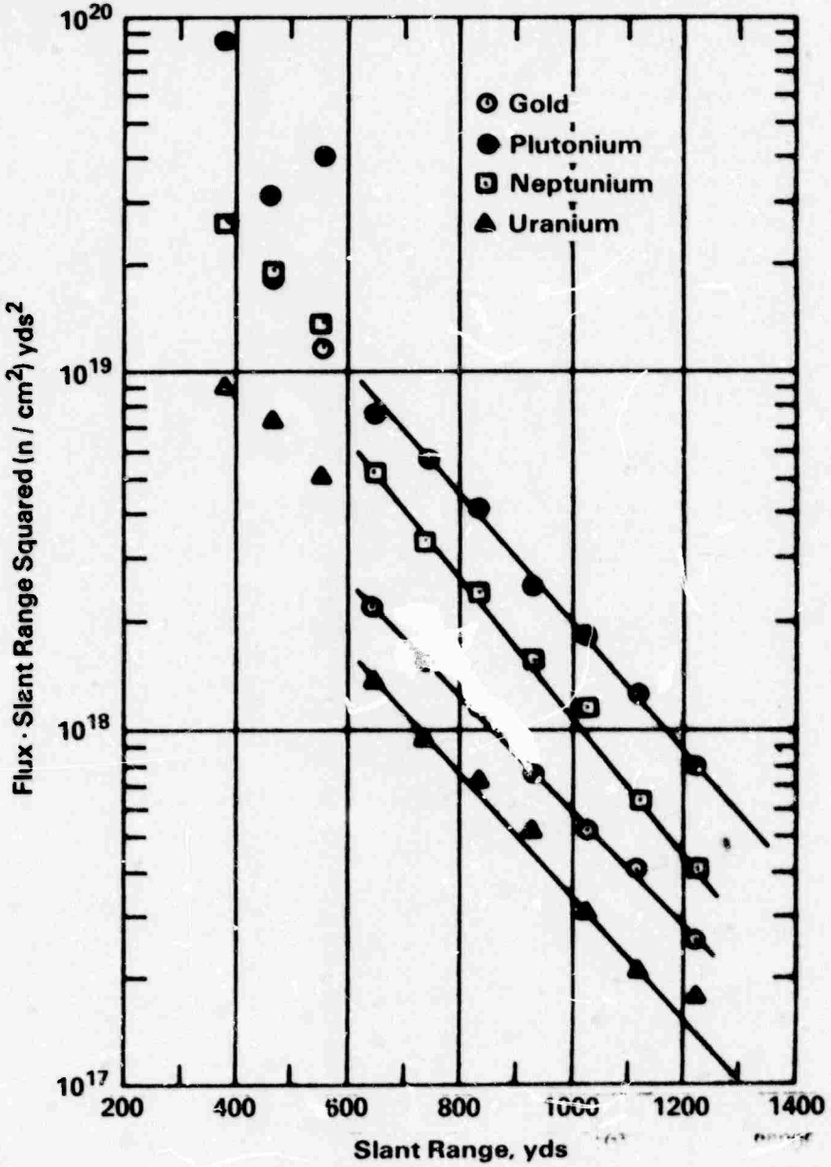

Figure 3.4 Neutron-Threshold-Detector Results, Shot Priscilla.

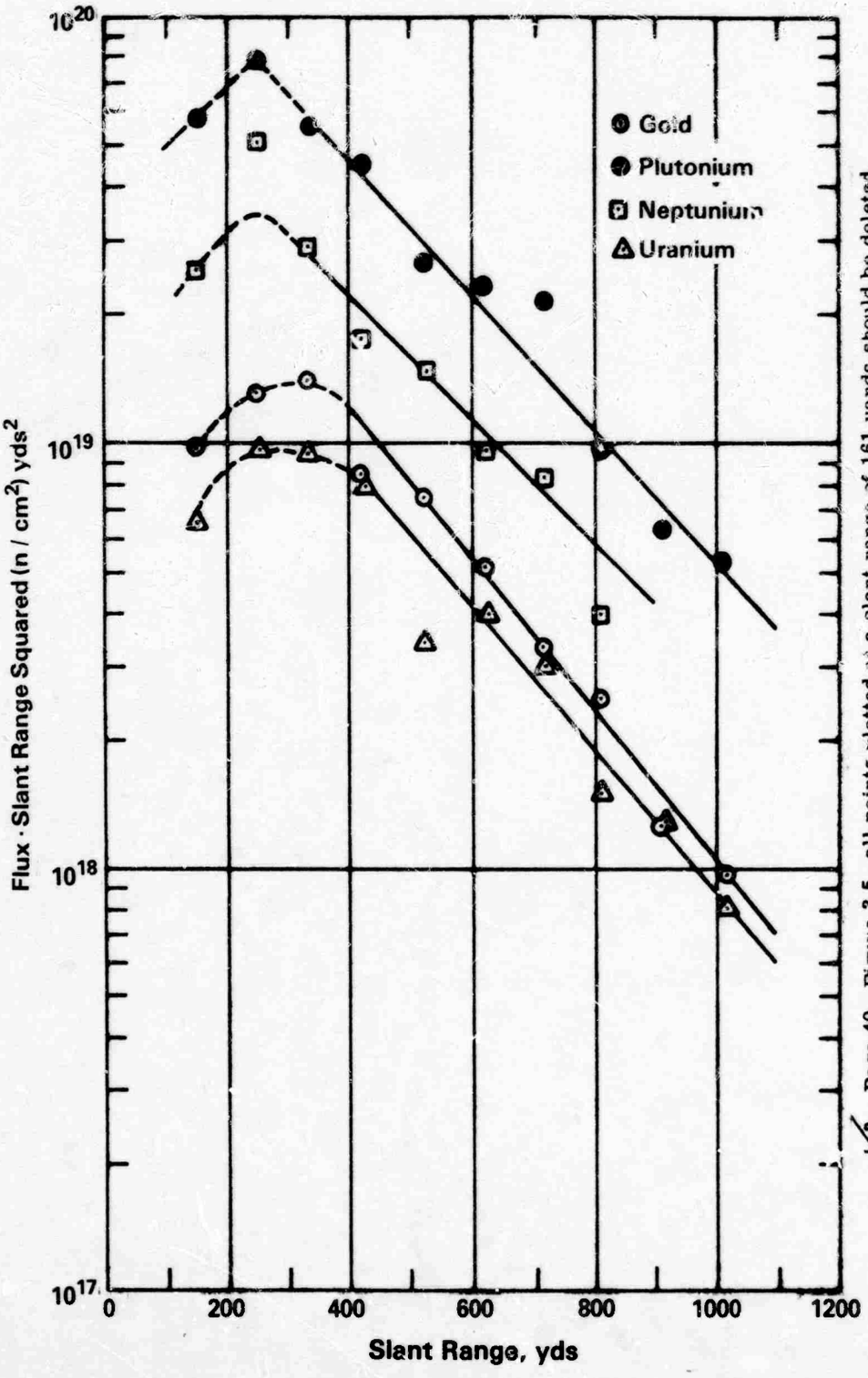

Figure 3.5 Neutron-Threshold-Detector Results, Shot Owens.

3. Page 40, Figure 3.5, all points plotted at a slant range of 161 yards should be deleted and replaced by:

Detector	Slant Range yd	Flux times Slant Range Squared
Au	195	1.43×10^{19}
Pu	195	8.48×10^{18}
Np	195	3.73×10^{18}
U	195	9.66×10^{18}

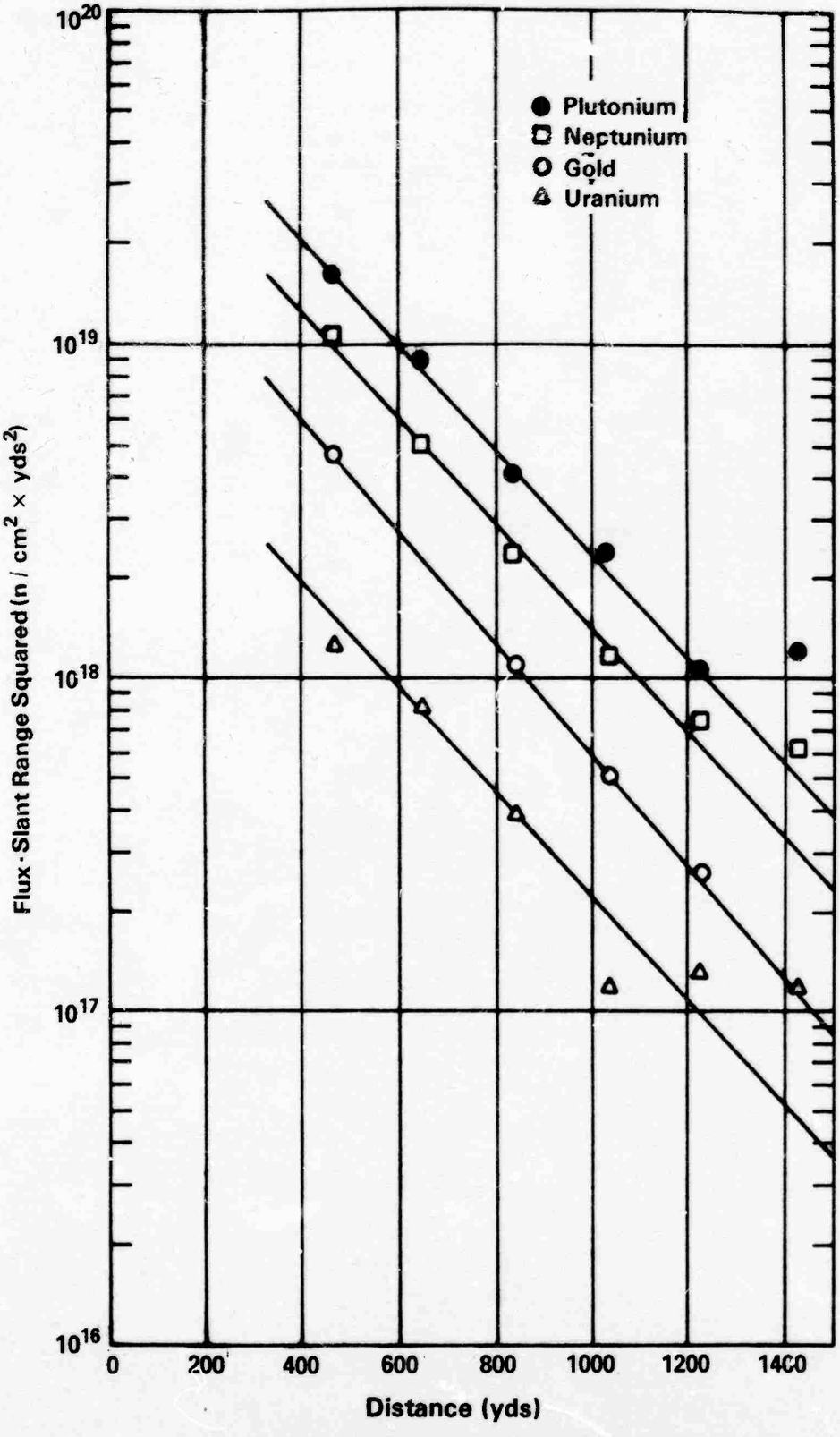

Figure 3.6 Neutron-Threshold-Detector Results for 167-Degree Line, Shot Smoky.

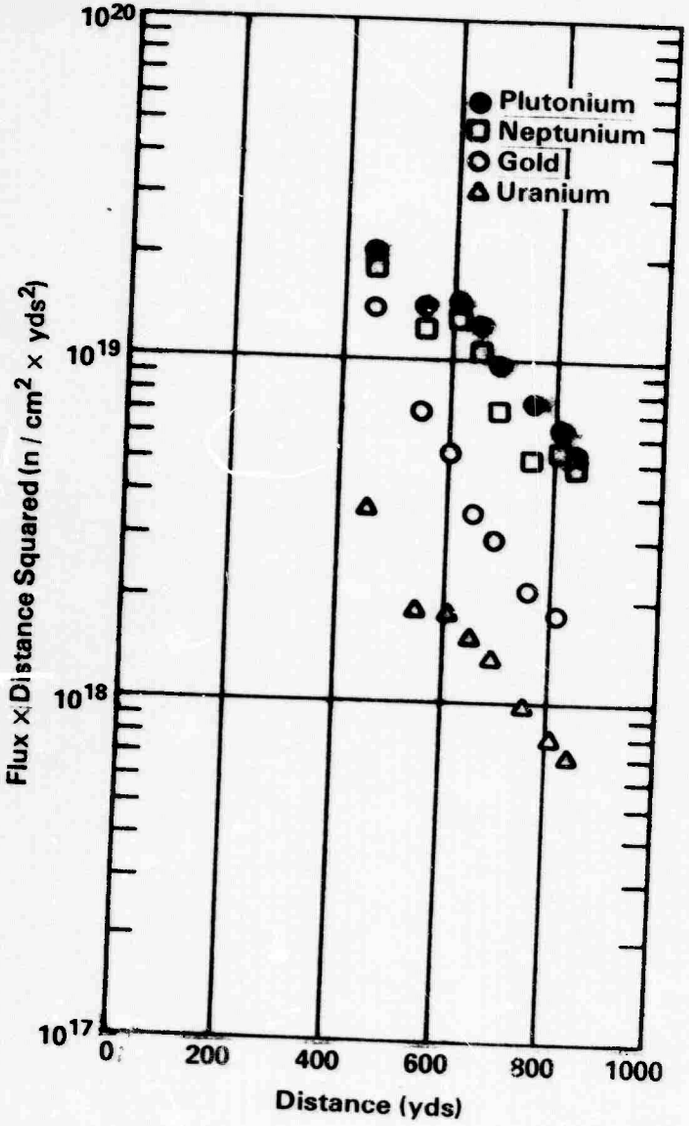

Figure 3.7 Neutron-Threshold-Detector Results for 58-Degree Line, Shot Smoky.

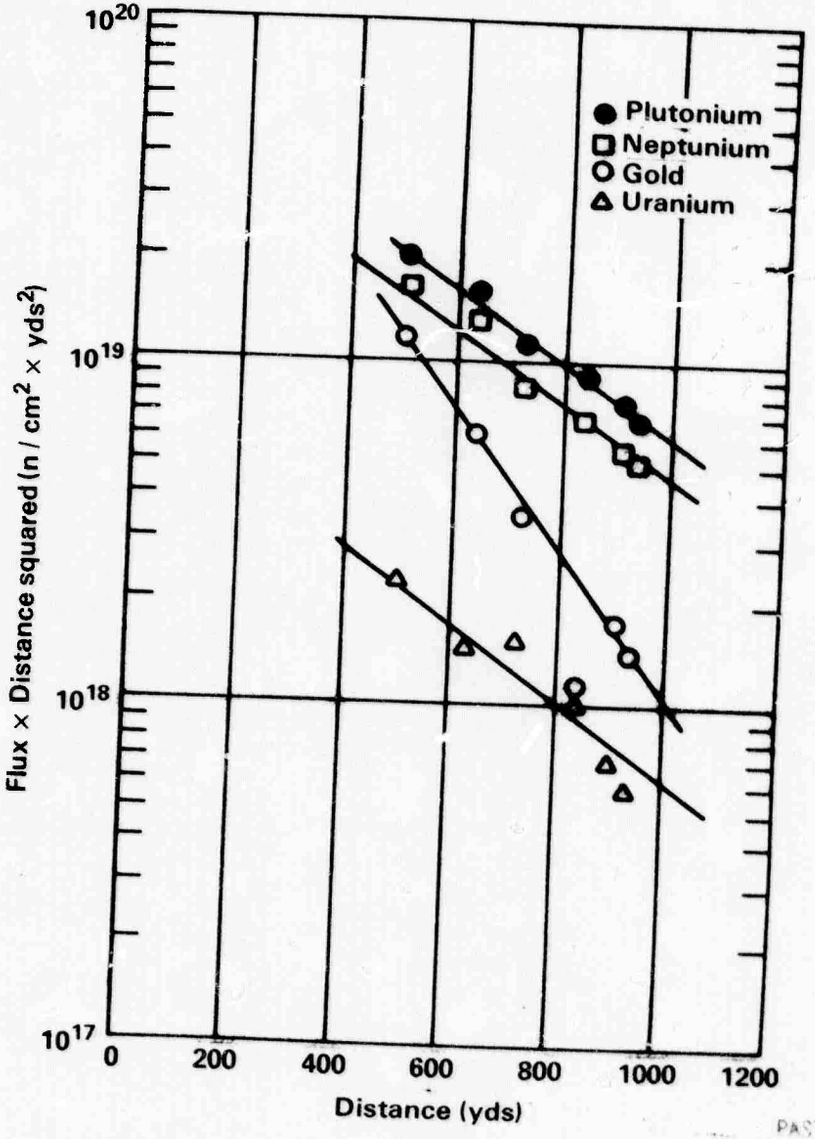

Figure 3.8 Neutron-Threshold-Detector Results for 353-Degree Line, Shot Smoky.

counted at various times after irradiation up to H + 300 hours. The flux was calculated in the usual way from the 20 hour calibration number. The results of neutron measurements made on this shot by CETG Project 39.5 are not available.

The data obtained using the USAF chemical dosimeters may be found in Reference 18.

3.1.9 Shot Laplace. Results of the neutron flux measurements from Shot Laplace are presented in Table 3.8. Figure 3.9 shows plots of flux versus slant range.

Results of the study of variation of gold fluxes with soil depth obtained by the Naval Radiological Defense Laboratories are given in Table 3.9.

3.2 NEUTRON DOSE

Equation 1.1 was utilized in the calculation of the tissue dose in rep from the neutron flux determinations. However, due to the small amounts of neptunium used in the neptunium samples, the resultant activity was, in many cases, too low to be measured. In these cases, the following equation was used to determine the dose in rep:

$$D = \left[1.8\,(N_{Pu} - N_U) + 3.2\,(N_U - N_S) + 3.9\,(N_S) \right] \times 10^{-9} \qquad (3.1)$$

where the coefficients were determined from the first collision dose curve at the average energies between the respective thresholds, just as they were in Equation 1.1. The thermal neutron term was omitted in this expression, as its contribution to the dose was negligible.

The neutron dose measurements from Shots Franklin, Wilson, Priscilla, Owens, Smoky, and Laplace are given in Tables 3.10, 3.11, 3.12, 3.13, 3.14, and 3.15, respectively. Plots of neutron dose times the square of the slant range versus the slant range for these shots are shown in Figures 3.10, 3.12, 3.14, 3.16, 3.18, and 3.21, respectively.

Neutron dose results are presented for two sets of meteorological conditions: (1) as measured at the conditions: (1) as measured at the conditions shown in Table 3.16, and (2) as corrected to the conditions of a relative air density of unity (in units of 1.22×10^{-3} gm-cm^{-3}, the density of average atmospheric air at 1,013 millibars pressure and 15C temperature). Because the interpretation of previous experimental data have indicated that the perturbations of the flux due to atmospheric water vapor are much less than the error in the measurements themselves, the effect of water vapor content was neglected. Thus, the corrected data reported herein may be compared directly with the data reported for the various tests conducted at the EPG since the meteorological conditions there are similar to the standard conditions chosen for unit air density.

The above mentioned corrections are made by means of the following formulae and relations:

$$\bar{\rho} = 0.284\,\frac{P}{T} \qquad (3.2)$$

$$\bar{\rho}_1 R_1 = \bar{\rho}_2 R_2 \qquad (3.3)$$

$$\varphi_2 = \left(\frac{\bar{\rho}_2}{\rho_1} \right)^2 \varphi_1 \qquad (3.4)$$

Where: $\bar{\rho}$ = relative air density

P = ambient atmospheric pressure, millibars

T = ambient atmospheric temperature, degrees K

R = slant range from device to detector, yards

φ = neutron dose, rep

Equation 3.2 was used to calculate the relative air densities for the conditions under which each device was detonated. Theoretical and correlational considerations necessitate that both Equa-

Text continued on Page 53.

TABLE 3.8 RESULTS OF NEUTRON-THRESHOLD-DETECTOR MEASUREMENTS, SHOT LAPLACE

Station Number	Slant Range	Measured Flux			
		Au	Pu	Np	U
	yds	n/cm^2	n/cm^2	n/cm^2	n/cm^2
7-2.10-9002.01	270	1.70×10^{13}	6.04×10^{13}	2.83×10^{13}	4.78×10^{12}
7-2.10-9002.02	324	—	—	—	—
7-2.10-9002.03	390	6.31×10^{12}	1.88×10^{13}	1.02×10^{13}	1.66×10^{12}
7-2.10-9002.04	470	—	—	—	—
7-2.10-9002.04A	510	2.54×10^{12}	6.65×10^{12}	3.52×10^{12}	6.49×10^{11}
7-2.10-9002.04A	510	2.16×10^{12}	—	—	—
7-2.10-9002.05	558	1.81×10^{12}	4.76×10^{12}	2.55×10^{12}	4.48×10^{11}
7-2.10-9002.06	650	—	—	—	—
7-2.10-9002.07	742	4.27×10^{11}	1.27×10^{12}	6.94×10^{11}	1.10×10^{11}
7-2.10-9002.08	837	—	—	—	—
7-2.10-9002.09	934	1.31×10^{11}	3.75×10^{11}	—	4.27×10^{10}
7-2.10-9002.10	1,030	—	—	—	—
7-2.10-9002.11	1,128	3.64×10^{10}	1.02×10^{11}	—	1.19×10^{10}

TABLE 3.9 DEPTH MEASUREMENTS, SHOT LAPLACE 510 YARDS SLANT RANGE

Location of Sample with Respect to Soil Surface Level	Measured Flux
	Au
in	n/cm^2
4 Above	—
2 Above	3.56×10^{12}
3/4 Below	3.82×10^{12}
2 1/4 Below	4.40×10^{12}
3 3/4 Below	4.46×10^{12}
4 Below	—
5 1/4 Below	4.18×10^{12}
6 Below	4.10×10^{12}
6 3/4 Below	3.63×10^{12}
8 1/4 Below	3.08×10^{12}
9 3/4 Below	2.42×10^{12}
11 1/4 Below	2.02×10^{12}
13 Below	—
15 Below	1.30×10^{12}
22 Below	—
24 Below	2.45×10^{11}

TABLE 3.10 NEUTRON DOSE, SHOT FRANKLIN

Station Number	$\bar{\rho}$ = 0.84		$\bar{\rho}$ = 1.0	
	Slant Range	Dose	Slant Range	Dose
	yds	rep	yds	rep
3-2.3-9001.01	158	2.49×10^{4}	133	3.54×10^{4}
3-2.3-9001.02	218	1.33×10^{4}	183	1.89×10^{4}
3-2.3-9001.03	327	3.55×10^{3}	275	5.04×10^{3}
3-2.3-9001.04	437	1.41×10^{3}	367	2.00×10^{3}

TABLE 3.11 NEUTRON DOSE, SHOT WILSON

Station Number	$\bar{\rho}$ = 0.64		$\bar{\rho}$ = 1.0	
	Slant Range	Dose	Slant Range	Dose
	yds	rep	yds	rep
9-41-7001.03	356	3.60×10^5	301	5.11×10^5
9-41-7001.07	600	5.74×10^4	504	6.15×10^4
9-41-7001.12	924	6.48×10^3	776	9.20×10^3
9-41-7001.16	1,220	1.16×10^3	1,025	1.65×10^3

TABLE 3.12 NEUTRON DOSE, SHOT PRISCILLA

Station Number	$\bar{\rho}$ = 0.65		$\bar{\rho}$ = 1.0	
	Slant Range	Dose	Slant Range	Dose
	yds	rep	yds	rep
F-2.3-9009.03	380	9.27×10^5	323	1.26×10^5
F-2.3-9009.04	463	3.13×10^5	394	4.32×10^5
F-2.3-9009.05	552	2.15×10^5	469	2.97×10^5
F-2.3-9009.06	644	4.07×10^4	547	5.62×10^4
F-2.3-9009.07	736	$2.[illegible] \times 10^4$	627	2.96×10^4
F-2.3-9009.08	833	1.23×10^4	706	1.70×10^4
F-2.3-9009.09	930	6.19×10^3	791	6.54×10^3
F-2.3-9009.10	1,027	3.27×10^3	873	4.51×10^3
F-2.3-9009.11	1,124	1.94×10^3	955	2.66×10^3
F-2.3-9009.12	1,222	1.05×10^3	1,039	1.45×10^3

TABLE 3.13 NEUTRON DOSE, SHOT OWENS

Station Number	$\bar{\rho}$ = 0.62		$\bar{\rho}$ = 1.0	
	Slant Range	Dose	Slant Range	Dose
	yds	rep	yds	rep
9-2.3-9004.12	~~181~~ 195	3.95×10^5	~~182~~ 160	5.89×10^5
9-2.3-9004.13	250	2.47×10^5	213	3.66×10^5
9-2.3-9004.14	343	9.12×10^5	281	1.36×10^5
9-2.3-9004.15	433	4.27×10^5	355	6.36×10^5
9-2.3-9004.16	527	1.92×10^5	432	2.66×10^5
9-2.3-9004.17	623	1.08×10^5	511	1.60×10^5
9-2.3-9004.18	720	7.17×10^4	590	1.07×10^5
9-2.3-9004.19	817	2.61×10^4	670	3.69×10^4
9-2.3-9004.20	915	—	750	—
9-2.3-9004.21	1,014	—	831	—

TABLE 3.14 NEUTRON DOSE, SHOT SMOKY

Station Number	Distance from Ground Zero	Azimuth	$\bar{\rho}$ = 0.63		$\bar{\rho}$ = 1.0	
			Slant Range	Dose	Slant Range	Dose
	yds	deg	yds	rep	yds	rep
400 S	400	167	466	1.85×10^5	367	2.24×10^5
600 S	600		649	4.17×10^4	539	6.04×10^4
600 S	600		641	1.15×10^4	696	1.67×10^4
1,000 S	1,000		1,034	4.13×10^3	856	5.99×10^3
1,200 S	1,200		1,229	1.56×10^3	1,020	2.26×10^3
1,400 S	1,400		1,426	1.12×10^3	1,164	1.62×10^3
450 N	450	353	496	1.92×10^5	413	2.76×10^5
600 N	600		629	9.57×10^4	522	1.39×10^5
700 N	700		719	5.00×10^4	597	7.25×10^4
625 N	625		633	2.93×10^4	691	4.25×10^4
900 N	900		903	2.04×10^4	749	2.96×10^4
930 N	930		933	1.74×10^4	774	2.52×10^4
400 E	400	56	456	2.47×10^5	360	3.58×10^5
500 E	500		545	1.16×10^5	452	1.66×10^5
565 E	565		607	9.92×10^4	504	1.44×10^5
605 E	605		657	7.09×10^4	545	1.03×10^5
660 E	660		691	4.52×10^4	573	6.55×10^4
725 E	725		756	2.82×10^4	627	4.09×10^4
780 E	780		610	2.32×10^4	[illegible]	3.36×10^4
610 E	810		641	1.66×10^4	696	2.73×10^4

TABLE 3.15 NEUTRON DOSE, SHOT LAPLACE

Station Number	$\bar{\rho}$ = 0.64		$\bar{\rho}$ = 1.0	
	Slant Range	Dose	Slant Range	Dose
	yds	rep	yds	rep
7-2.10-9002.01	270	1.07×10^5	227	1.52×10^5
7-2.10-9002.03	390	3.56×10^4	327	5.06×10^4
7-2.10-9002.04A	510	1.24×10^4	426	1.76×10^4
7-2.10-9002.05	556	9.00×10^3	469	1.26×10^4
7-2.10-9002.07	742	2.41×10^3	623	3.42×10^3

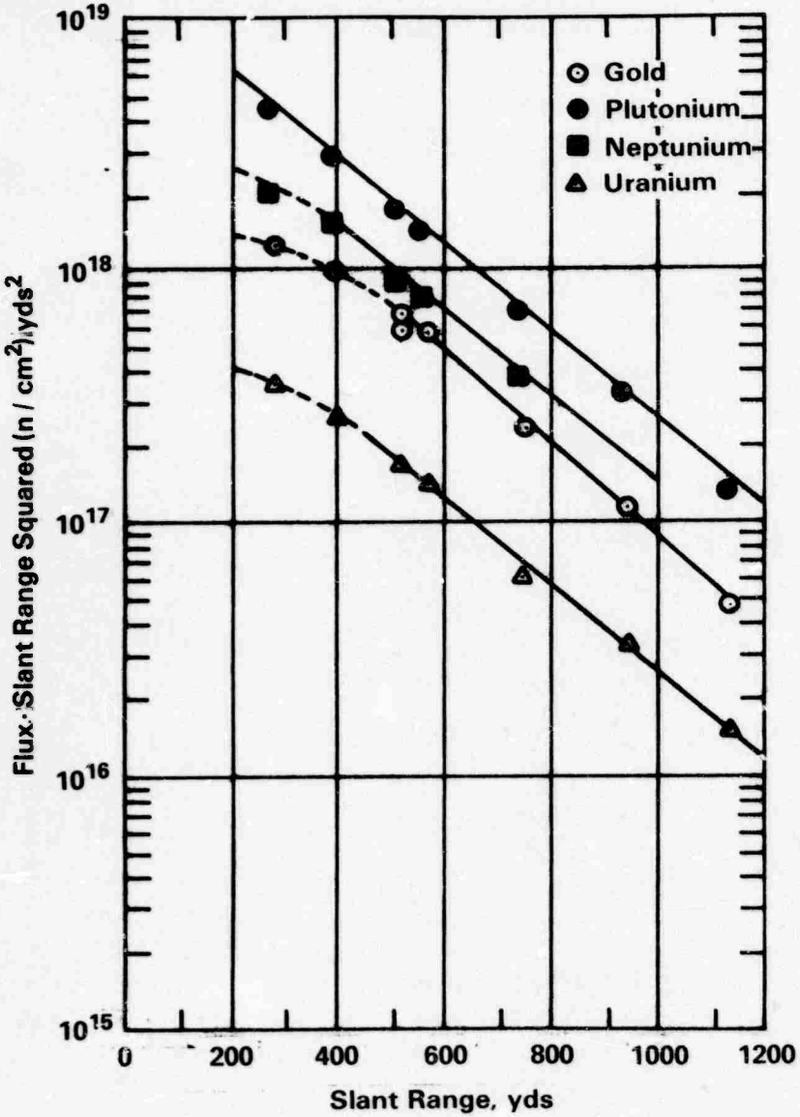

Figure 3.9 Neutron-Threshold-Detector Results, Shot Laplace.

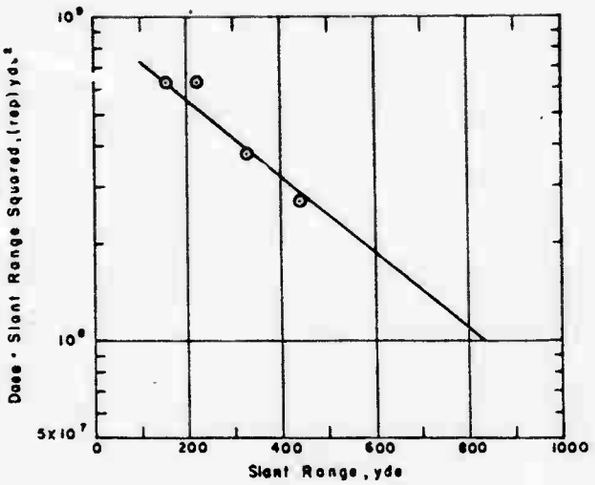

Figure 3.10 Neutron-threshold-detector dose distance squared versus distance for Shot Franklin.

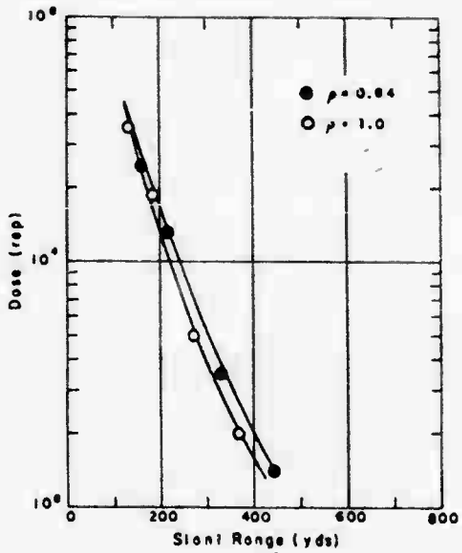

Figure 3.11 Neutron-threshold-detector dose versus distance for Shot Franklin.

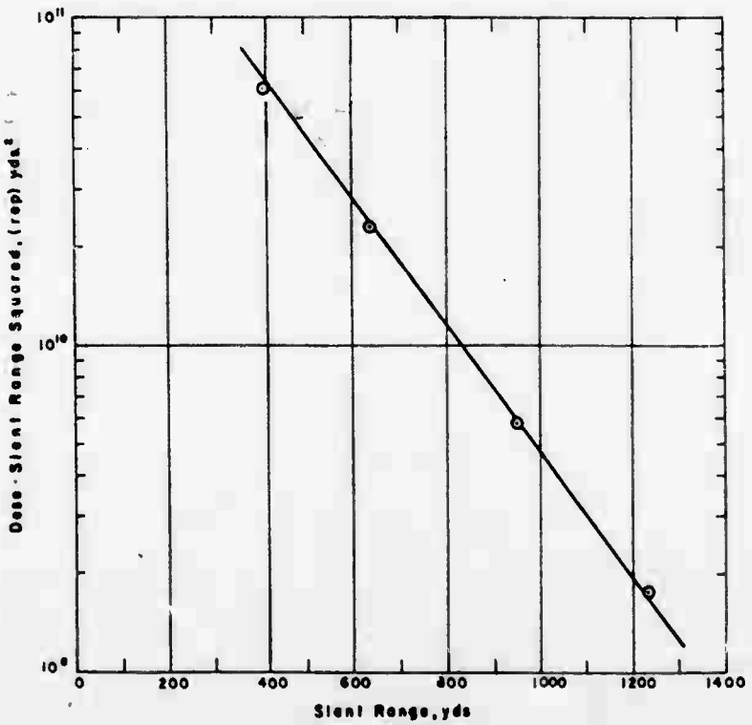

Figure 3.12 Neutron-threshold-detector dose distance squared versus distance for Shot Wilson.

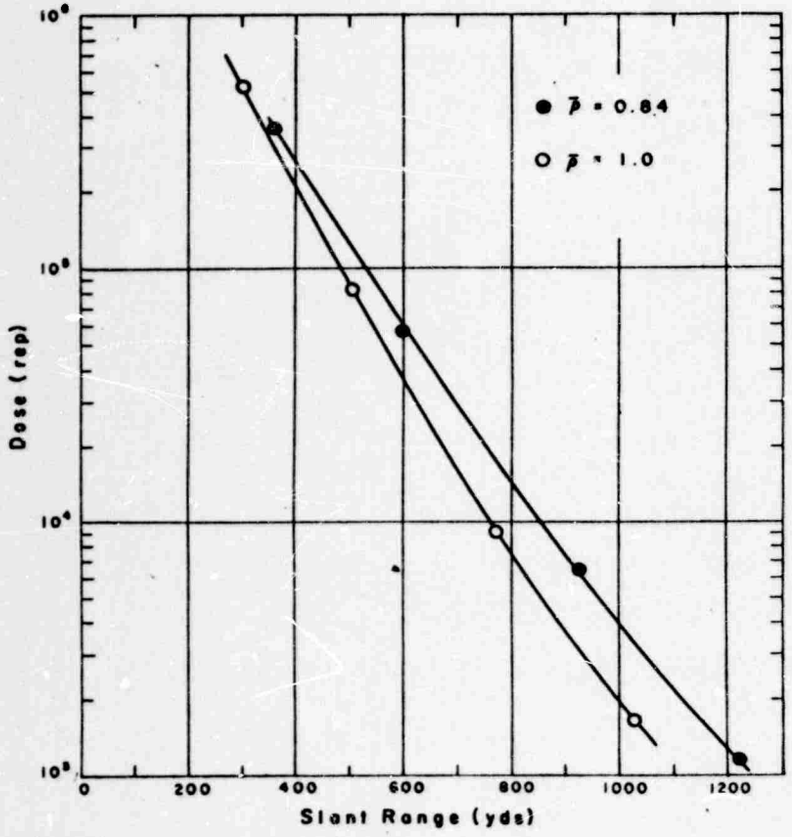

Figure 3.13 Neutron-threshold-detector dose versus distance for Shot Wilson.

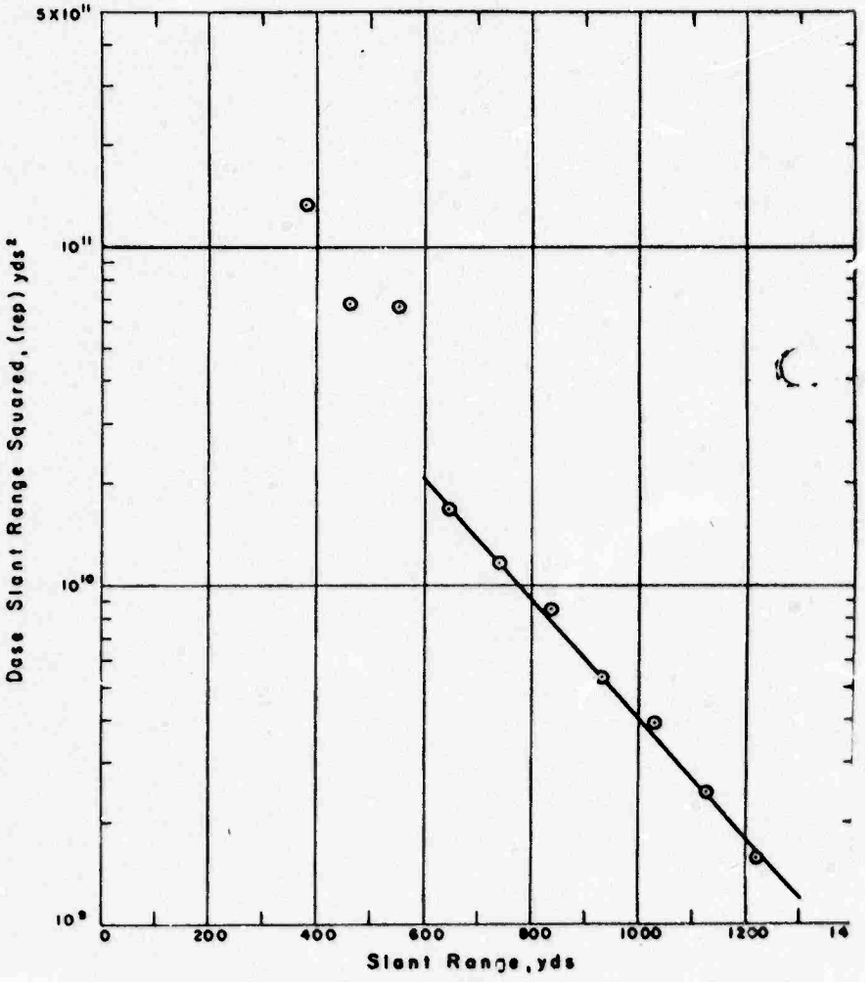

Figure 3.14 Neutron-threshold-detector dose distance squared versus distance, Shot Priscilla.

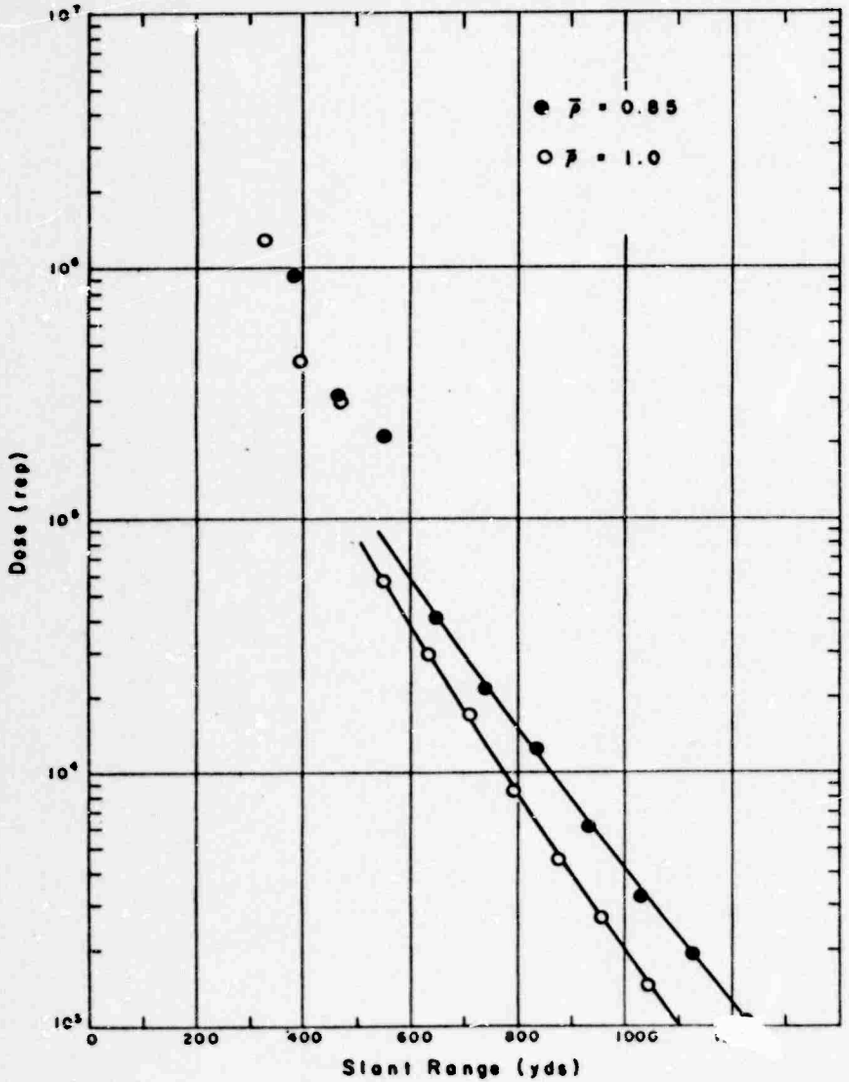

Figure 3.15 Neutron-threshold-detector dose versus distance, Shot Priscilla.

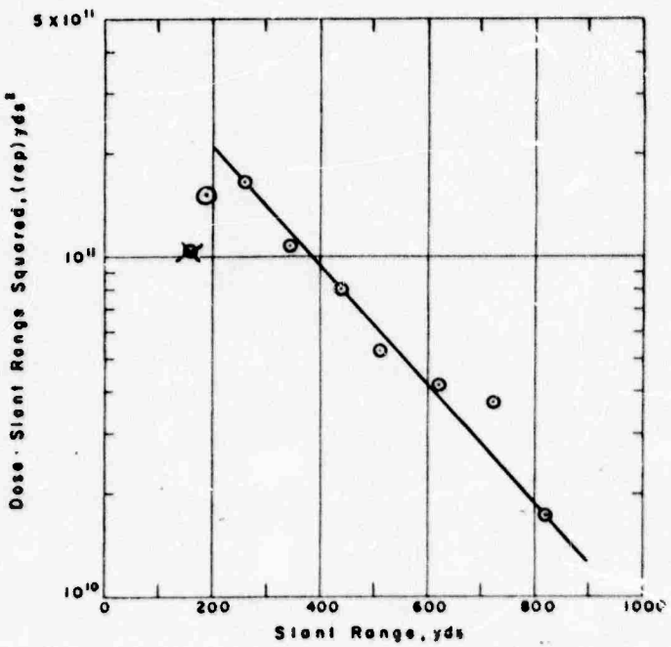

Figure 3.16 Neutron-threshold-detector dose distance squared versus distance, Shot Owens.

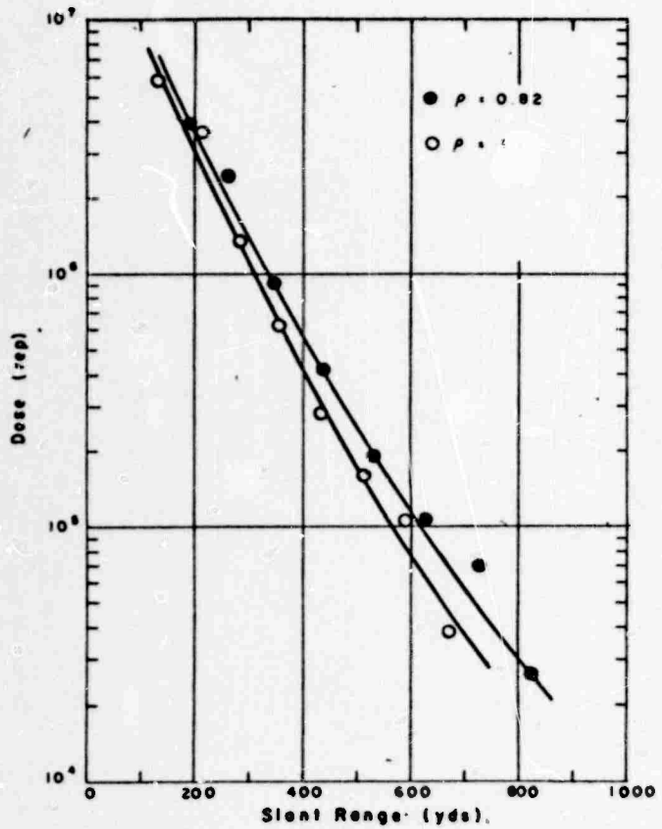

Figure 3.17 Neutron-threshold-detector dose versus distance, Shot Owens.

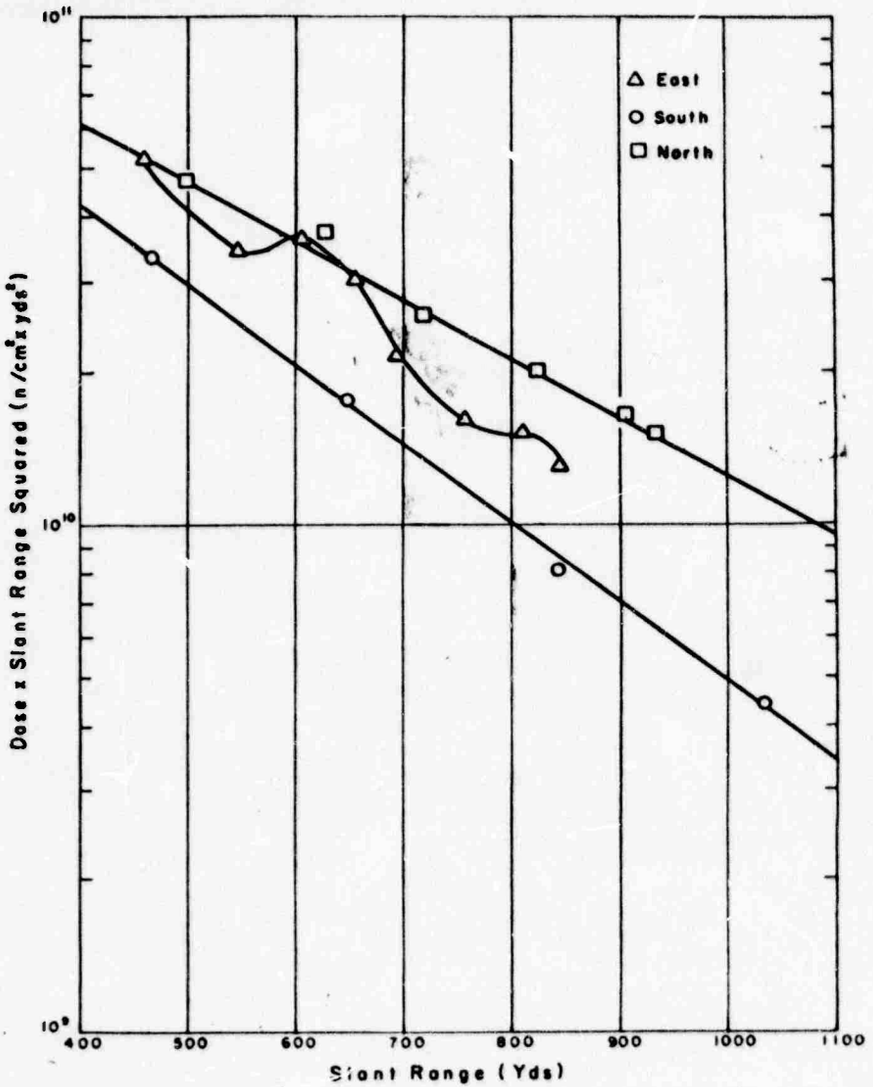

Figure 3.18 Neutron-threshold-detector dose distance squared versus distance, Shot Smoky.

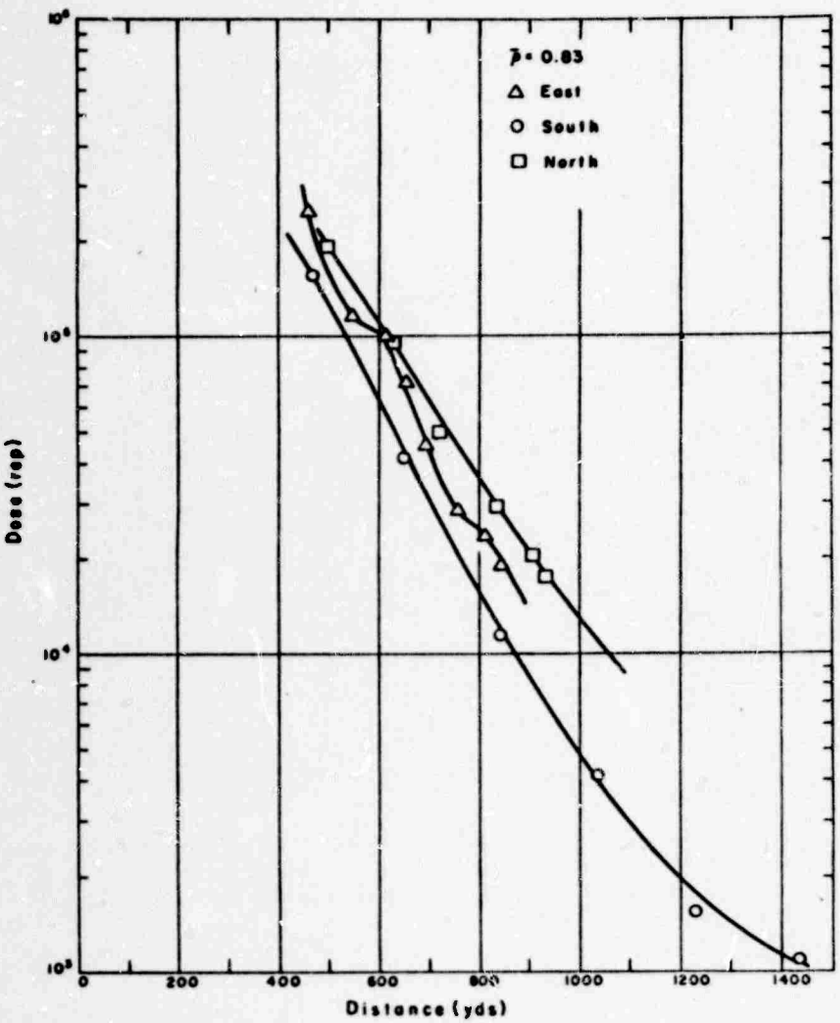

Figure 3.19 Neutron-threshold-detector dose versus distance, Shot Smoky.

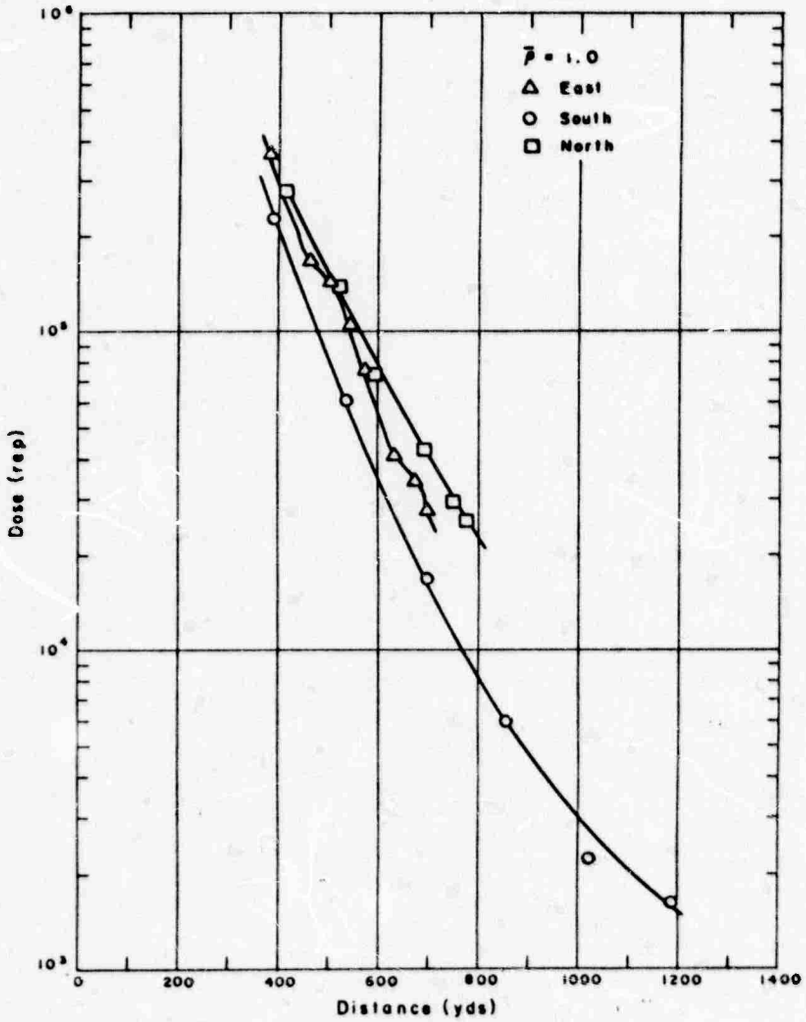

Figure 3.20 Neutron-threshold-detector dose versus distance, Shot Smoky.

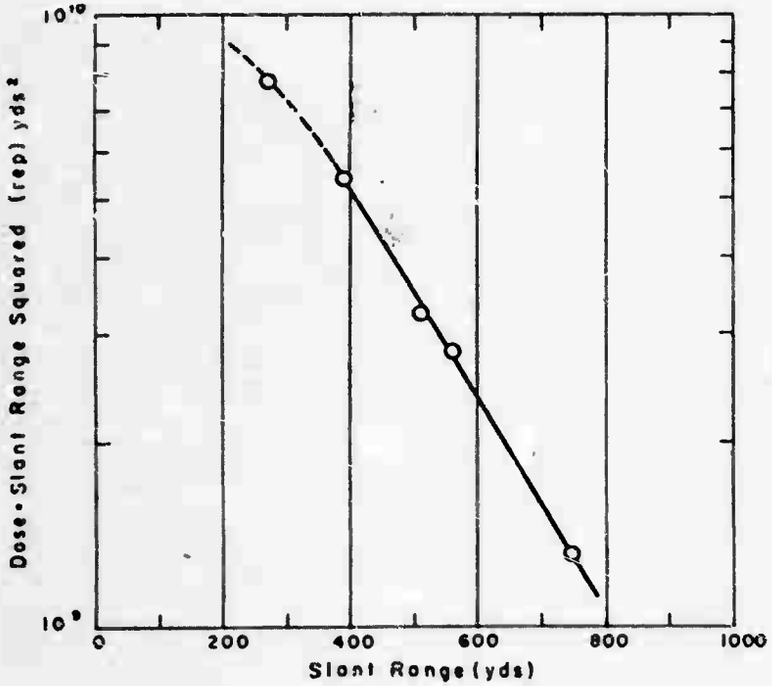

Figure 3.21 Neutron-threshold-detector dose distance squared versus distance, Shot Laplace.

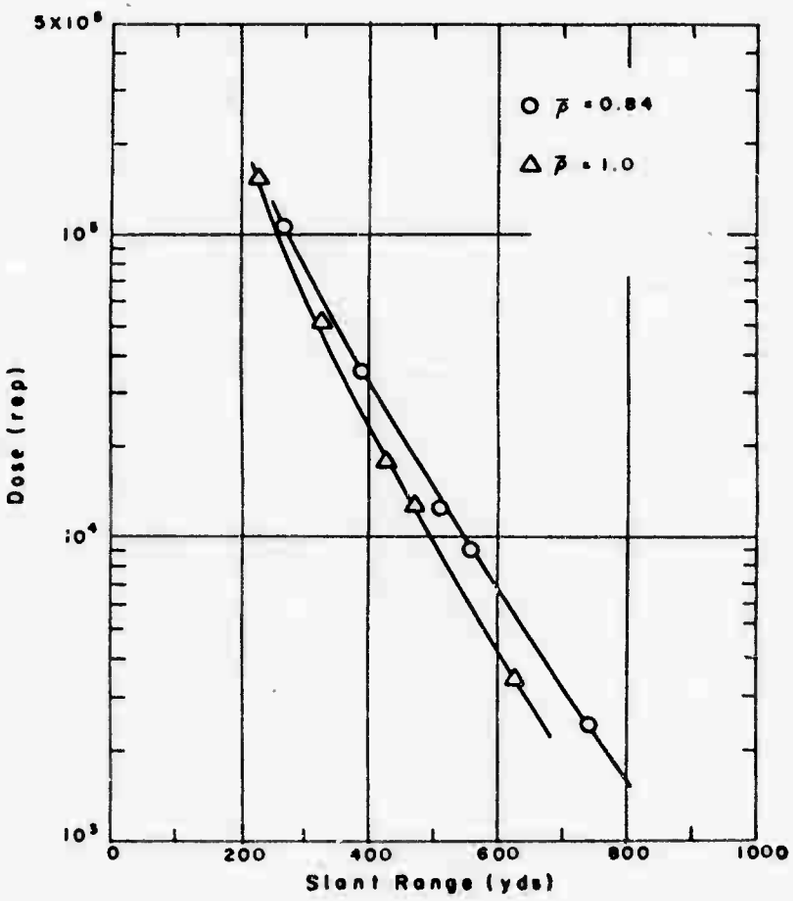

Figure 3.22 Neutron-threshold-detector dose versus distance, Shot Laplace.

tions 3.3 and 3.4 be satisfied in the calculation of the doses corrected to unity air density.

Plots of dose versus slant range at the two meteorological conditions are shown in Figures 3.11, 3.13, 3.15, and 3.17 for Shots Franklin, Wilson, Priscilla, and Owens; in Figures 3.19 and 3.20 for Shot Smoky; and in Figure 3.22 for Shot Laplace.

Chapter 4
DISCUSSION

4.1 NEUTRON FLUX AND SPECTRUM

As has been previously mentioned in Chapter 3, neutron spectrum for neutron energies above the thermal range was not expected to change with distance beyond 300 yards from ground zero, and it would follow from this assumption that a plot of the neutron flux versus distance for various energy ranges would show parallel lines. That this is indeed true is evidenced by the data obtained from Shots Franklin, Lassen, Wilson, Owens, and Laplace.

However, on Shot Priscilla, a variation from the predicted parallel-line-constant-spectrum concept was noted at the three stations at less than 500 yards from ground zero. Here, the placement of the detectors appeared to be the disturbing factor. These three stations were placed among many structures and other installations, which may have caused scattering and other disturbances in the flux field. These measurements, although an indication of the actual flux at the point of measurement, probably did not give a true picture of the free-field flux. If the free-field flux at these points is desired, the value taken from the extrapolation of the lines drawn through the other points probably gives a more realistic figure.

4.2 NEUTRON DOSE

Although most of the dose data presented in this report was calculated from Equation 1.1, in those cases where Np^{237} data was not available the dose data was calculated using Equation 3.1. This was due to the limited availability of neptunium samples. Generally, data which was calculated by this method was less than 10 percent higher than the data calculated by Equation 1.1.

In order to compare the total dose figures obtained during Operation Plumbbob with current prediction techniques, the dose per unit yield at various slant ranges was calculated and is presented in Table 4.1. Also presented are the predicted dosages at these same slant ranges taken from the plot of neutron radiation versus slant range for fission weapons as found in TM 23-200 (Reference 24).

In order to directly compare the predicted values with the current data, an rbe of 1.3, i.e., 1 rep = 1.3 rem (Reference 24), and a relative air density of 1.0 were used. Figure 4.1 shows a plot of these values. It is stated in TM 23-200 that the prediction curve may be low by as much as a factor of four for certain experimental devices and as high as a factor of 10 for other devices. It is apparent from the plot that the data from Shots Laplace, Franklin, Wilson, and Priscilla fall within these factors of reliability, while that from Shot Owens is above the factor of reliability. Specifically, the average ratio between measured and predicted values over the distances for which measurements were made were: Priscilla = 0.8; Franklin = 2.4; Wilson = 2.9; Laplace = 3.0; and Owens = 5.6.

It should be noted however that there was a variation of thickness of high explosive surrounding the core of the devices listed in Table 4.1. Although the differences in the dose per unit yield for the devices tested may be in part due to the variance in the thickness of high explosive, no basis has been found to directly correlate these two parameters.

4.3 EFFECT OF TERRAIN ON NEUTRON FLUX AND DOSE

A quantitative evaluation of the effect of terrain on neutron flux based on the data obtained from Shot Smoky is impossible due to the design of the device.

[redacted] Although the north line, which was run to the top of a high hill, showed higher flux values than the south line which was run along level terrain, it would be extremely presumptuous to attribute these higher values to the particular terrain feature in question. The east line exhibited a definite variation which could be attributed to the rolling terrain. However, no quantitative measurement of this effect was possible. This data as it applies to the effect of terrain on neutron flux can be considered inconclusive at best.

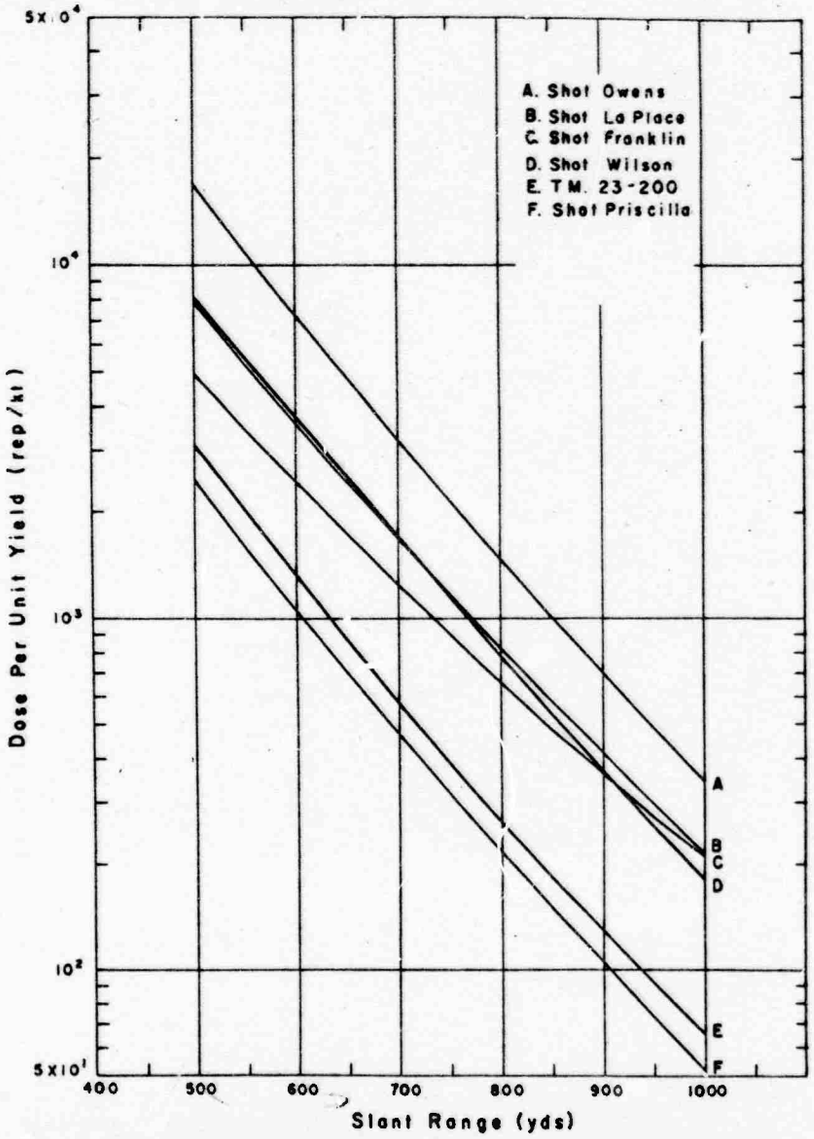

Figure 4.1 Dose per unit yield of various devices compared with current predictions information.

4.4 DATA RELIABILITY

The errors expected in the measurement of neutron flux in this report are discussed in Section 2.2.6, which gives the details of the calibration procedures. The error in the measurement of neutron dose in rep can most easily be estimated by comparison with some other method. The fission-foil method of measuring neutron dose was developed as a field expedient for the Hurst proportional counter (Reference 13). The foils and calibration numbers have been cross checked with other agencies using the fission-foil method for measuring dose. A comparison of the data obtained by these agencies generally agreed within 10 percent.

The experimental variation in the neutron flux and dose data is shown in Table 4.2. This table compares two sets of detectors exposed to Shot Hood. One set of detectors was on the east side of the Project 2.4 tank array and the other on the west side, both being at the same radial distance from ground zero and with a ground separation of approximately 60 yards. The

TABLE 4.1 DOSE PER UNIT YIELD OF VARIOUS DEVICES COMPARED WITH CURRENT PREDICTION INFORMATION

Slant Range yds	Dose per Unit Yield, rep/kt *					
	Franklin †	Wilson ‡	Priscilla §	Owens ¶	Laplace **	TM 23-200 ††
500	4.90×10^3	8.07×10^3	2.46×10^3	1.66×10^4	7.80×10^3	3.08×10^3
600	2.37×10^3	3.55×10^3	1.02×10^3	6.93×10^3	3.48×10^3	1.31×10^3
700	1.21×10^3	1.65×10^3	4.59×10^2	3.14×10^3	1.65×10^3	5.38×10^2
800	6.57×10^2	7.67×10^2	2.13×10^2	1.45×10^3	8.19×10^2	2.61×10^2
900	3.63×10^2	3.63×10^2	1.03×10^2	6.96×10^2	4.14×10^2	1.23×10^2
1,000	2.07×10^2	1.77×10^2	5.13×10^1	3.46×10^2	2.13×10^2	6.50×10^1

* All values based or a relative air density of 1.0

[redacted]

†† Based on an RBE of 1.3.

TABLE 4.2 COMPARISON OF DUPLICATE STATIONS ON SHOT HOOD

Sample Type	Measured	Average	Variation from Average	Percent Variation
Flux:	n/cm^2	n/cm^2	n/cm^2	
Au	3.59×10^{12} 4.01×10^{12}	3.80×10^{12}	0.21×10^{12}	5.53
Pu	1.64×10^{13} 1.68×10^{13}	1.66×10^{13}	0.02×10^{13}	1.20
Np	1.04×10^{13} 1.24×10^{14}	1.10×10^{13}	0.10×10^{13}	9.09
U	2.93×10^{12} 2.81×10^{12}	2.87×10^{12}	0.05×10^{12}	2.09
[redacted]				
Dose:	rep	rep	rep	
	3.11×10^4 3.41×10^4	3.26×10^4	0.15×10^4	4.60

large variation in neptunium flux is attributed to the inaccurate weights of the neptunium samples. The weights of these samples are accurate only to three significant figures, while the plutonium and uranium sample weights are accurate to five significant figures. This is due to the fact that the neptunium samples weigh only 25 to 30 mg, whereas the plutonium and uranium samples all have weights over 1 gram.

4.5 EFFECTIVENESS OF INSTRUMENTATION

The instrumentation used in these tests has proven effective in measuring neutron dose. The necessity for early recovery of the fission foils is still a disadvantage. However, when fallout is light in the immediate area of the detonation and when induced field intensities are low, this disadvantage is minimized. Even in cases when appreciable fallout is expected, the neutron detectors can be installed to take advantage of predicted upwind positions to permit early recovery without the necessity of entering high radiation fields. The continued use of the fission foil detectors will undoubtedly lead to improved techniques of recovery that will make the method more sensitive and increase the general effectiveness of the measurements of neutron flux and dose.

Chapter 5
CONCLUSIONS and RECOMMENDATIONS

5.1 CONCLUSIONS

For Shots Franklin, Wilson, Laplace, and Owens the measured dose values exceeded the predicted values obtained by use of the neutron dose curves of TM 23-200 by factors of 2.4, 2.9, 3.0, and 5.6, respectively. For Shot Priscilla, the measured dose was lower than the predicted dose by a factor of 1.2.

Beyond 300 yards from ground zero there was no variation of the neutron energy spectrum above the thermal energies with increasing distance from the point of detonation.

The extrapolation of the straight-line portion of the curve of neutron flux times slant distance squared versus the slant distance to close-in distances was invalid, since experimental data from Operation Plumbbob confirmed that the relationship was nonlinear at close ranges.

The foil-detector system for measuring neutron flux gave reproducible results, further verifying its suitability for use in making measurements during nuclear weapons tests.

5.2 RECOMMENDATIONS

No recommendations are made.

REFERENCES

1. C.W. Luke, Capt, USA, D.L. Rigotti, R. Fullwood, and D. Anderson; "Neutron-Flux Measurements"; Project 2.51, Operation Redwing, ITR-1313, January 1957; Chemical Warfare Laboratories, Army Chemical Center, Maryland; Secret Restricted Data.

2. Scientific Director's Report, Operation Sandstone, Volume 18, Annex R, Part K and Addendum, 1948; Secret Restricted Data.

3. W. Ogle, C. Cowan, et al.; Operation Ranger, Los Alamos Scientific Laboratory Report LAB-j-2095; "Neutron Measurements"; Secret Restricted Data.

4. J. Allred, et al.; "Neutron Measurements"; Preliminary Report of Group LAJ-3 Greenhouse, 1951; Secret Restricted Data.

5. T.D. Hanscome, et al.; "Neutron Flux Measurements"; Project 2.3, Operation Tumbler-Snapper, WT-524, 1952; Office of Naval Research, Washington, D.C.; Secret Restricted Data.

6. D.K. Willet, T.D. Hanscome, and L.W. Flagg; "Neutron Flux Measurements"; Project 2.3, Operation Upshot-Knothole, WT-720, 1953; Office of Naval Research, Washington, D.C.; Secret Restricted Data.

7. T.D. Hanscome, D.K, Willett, and A. Brodsky; "Neutron Flux Measurements"; Project 2.3, Operation Castle, WT-914, October 1955; Naval Research Laboratory, Washington, D.C.; Secret Restricted Data.

8. T.D. Hanscome and D.K. Willett; "Neutron Flux Measurements"; Project 2.2, Operation Teapot, ITR-1116, May 1955; U.S. Naval Research Laboratory, Washington, D.C.; Secret Restricted Data.

9. P.S. Harris, et al.; "Physical Measurement of Neutron and Gamma Radiation Dose From High Neutron Yield Weapons and Correlation of Dose with Biological Effect"; Project 39.7, Operation Teapot, ITR-1167, April 1955; Los Alamos Scientific Laboratories, Los Alamos, New Mexico; Secret Restricted Data.

10. W.A. Biggers and others; "External Neutron and Gamma Flux Measurements by Sample Activation"; Annex 1.5, Part II, Section 1, Operation Greenhouse, 1951; Los Alamos Scientific Laboratories, Los Alamos, New Mexico; Secret Restricted Data.

11. W.A. Biggers and others; "External Neutron Measurements with Threshold Detectors"; Project 17.1, Operation Upshot-Knothole, WT-826, March 1955; Los Alamos Scientific Laboratory, Los Alamos, New Mexico; Secret Restricted Data.

12. W.A. Biggers and others; "External Neutron Measurements"; Project 14.1, Operation Castle, WT-952, October 1955; Los Alamos Scientific Laboratory, Los Alamos, New Mexico; Secret Restricted Data.

13. G.S. Hurst, et al.; "Techniques of Measuring Neutron Spectrum with Threshold Detectors Tissue Dose Determination"; The Review of Scientific Instrument; Volume 27, No. 3, March 1956.

14. G.S. Hurst, R.H. Richie, and H.N. Wilson; Scientific Instrument 22, 981, 1951; Unclassified.

15. K.M. Case, F. deHoffman, and C. Placzek; "Introduction to the Theory of Neutron Diffusion"; Volume 1, June 1953; Los Alamos Scientific Laboratory, Los Alamos, New Mexico; Unclassified.

16. Samuel S. Holland, and Paul I. Richards; "Penetration of Neutrons in Air"; AFSWP – TR–55–27, September 1956; Secret Restricted Data.

17. C.W. Luke, Capt, USA, D.L. Rigotti, R. Fullwood, and D. Anderson; "Neutron-Flux Measurements"; Project 2.51, Operation Redwing, ITR–1313, Appendix A, January 1957; Chemical Warfare Laboratories, Army Chemical Center, Maryland; Secret Restricted Data.

18. S. Sigoloff, L.C. Logie, H.M. Borella, and J.E. Pickering; "Gamma Measurements Utilizing the USAF Chemical Dosimeter"; Project 39.1, Operation Plumbbob, ITR–1500, December 1957; U.S. Air Force School of Aviation Medicine, Randolph AFB, Texas; Confidential Formerly Restricted Data.

19. J.W. Kinch, D.L. Rigotti; "An Activation Type Neutron Detection System and its Calibration"; U.S. Army Chemical Warfare Laboratories, Army Chemical Center, Maryland (to be published); Confidential Formerly Restricted Data.

20. Robert C. Tompkins and others; "Attenuation of Gamma and Neutron Radiation by Armor, Soil, and Structures"; Project 2.4, Operation Plumbbob, ITR–1413, December 1957; U.S. Army Chemical Warfare Laboratories, Army Chemical Center, Maryland; Secret Restricted Data.

21. E.N. York, Capt, USAF, and others; "Initial Neutron and Gamma Air-Earth Interface Measurements"; Project 2.10, Operation Plumbbob, ITR–1419, December 1957; Air Force Special Weapons Center, Kirtland Air Force Base, Albuquerque, New Mexico; Confidential Formerly Restricted Data.

22. C.S. Cook and others; "Gamma Radiation from Neutron-Induced Radioactive Isotopes"; Project 2.2, Operation Plumbbob, ITR–1411, November 1957; U.S. Naval Radiological Defense Laboratory, San Francisco 24, California; Secret Restricted Data.

23. Kermit C. Kaericher, Capt, USAF, and James E. Banks, 1st Lt, USAF; "Nuclear Radiation received by Aircrews firing the MB-1 Rocket"; Project 2.9, Operation Plumbbob, ITR–1418, October 1957; Air Force Special Weapons Center, Kirtland Air Force Base, Albuquerque, New Mexico; Secret Formerly Restricted Data.

24. "Capabilities of Atomic Weapons"; TM 23-200, Revised Edition, November 1957, Confidential Restricted Data.